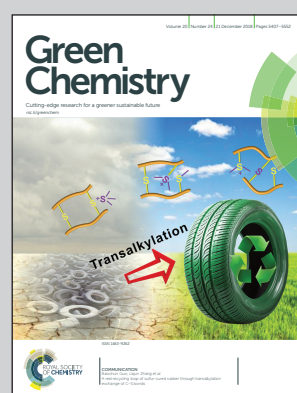


A critical review article presented by Mr Muhammad Sajid, Dr. Xuebing Zhao and Prof. Dr Dehua Liu of Department of Chemical Engineering, Tsinghua University, China.

Production of 2,5-furandicarboxylic acid (FDCA) from 5-hydroxymethylfurfural (HMF): recent progress focusing on the chemical-catalytic routes

The research progress on the production of 2,5-furandicarboxylic acid (FDCA) from bio-based platform chemical 5-hydroxymethylfurfural (HMF) has been comprehensively reviewed. Various oxidation routes and corresponding chemical mechanisms have been discussed in depth, focusing on the catalytic oxidation of HMF to FDCA under the catalysis of metal-based catalysts. However, although FDCA is an attractive chemical for bio-based polymer production, efforts have to be made with regards to the reaction kinetics and mechanisms as well as development of industrially-feasible processes.

### As featured in:



See Xuebing Zhao, Dehua Liu et al.,  
*Green Chem.*, 2018, **20**, 5427.



Cite this: *Green Chem.*, 2018, **20**, 5427

## Production of 2,5-furandicarboxylic acid (FDCA) from 5-hydroxymethylfurfural (HMF): recent progress focusing on the chemical-catalytic routes

Muhammad Sajid, <sup>a,b</sup> Xuebing Zhao \*<sup>a</sup> and Dehua Liu\*<sup>a</sup>

Furandicarboxylic acid (FDCA) has been considered as a good precursor, instead of petroleum-derived terephthalic acid (TPA), for producing green polymers such as polyethylene 2,5-furandicarboxylate (PEF). The production of FDCA from biomass or its derived sugars or platform chemicals generally involves chemical, biological and electrochemical methods, while the chemical-catalytic way seems to be the most promising in terms of the yield, reaction rate and product purity. The oxidative production of FDCA from bio-based 5-hydroxymethylfurfural (HMF) has attracted the most attention; it can be carried out by electrochemical, catalytic and non-catalytic processes. In the present work, we have comprehensively reviewed the current progress on the production of FDCA from HMF, primarily focusing on the chemical-catalytic approaches. The most frequently used catalysts for the chemical-catalytic methods are oxides of noble metals but their high cost, poor availability and recycling are the major hindrances to their commercial acceptance. Transition metal oxides are good alternatives but they suffer from relatively low FDCA yield. Electrochemical oxidation of HMF can be a good alternative route for FDCA production with simultaneous H<sub>2</sub> production but the yield and product recovery have to be further improved. Biocatalytic processes can produce FDCA with comparative yields under mild conditions but they can only be operated at low concentrations of HMF with much lower productivity. It is recommended that future works should be focused on, but not limited to, the comprehensive evaluation of different routes in terms of catalyst development and characterizations, process parameters, product yield and purity, as well as economic feasibility. The kinetics and reaction mechanisms of the process also need to be more deeply investigated to guide further process intensification.

Received 23rd August 2018,  
Accepted 23rd October 2018  
DOI: 10.1039/c8gc02680g  
[rsc.li/greenchem](http://rsc.li/greenchem)

## Introduction

The scale of the global economy has expanded many-fold to meet the continuously growing demands of energy, chemicals and materials. The chemical industry has also seen tremendous growth in the use of chemical intermediates, polymeric materials and integrated derivatives.<sup>1,2</sup> Conventionally, chemical industries rely heavily on fossil fuel-derived petrochemicals.<sup>3,4</sup> However, these petrochemicals are non-sustainable in terms of their supply, price and they cause global warming and environmental pollution.<sup>5,6</sup> These features of fossil fuel-derived chemicals have forced humans to search for more renewable and sustainable feedstocks.<sup>7,8</sup> Lignocellulosic biomass (LCB) is quite abundant in the natural world with a wide geographical distribution and can thus be explored to

produce green bio-based chemicals.<sup>9,10</sup> The U.S. Department of Energy in collaboration with the U.S. Department of Agriculture have indicated that there will be an increase in the commodities of biochemicals and bio-materials to 25% in 2030.<sup>11</sup> This goal has settled on the use of LCB as a renewable (in term of CO<sub>2</sub> balance) and sustainable resource of petroleum carbon for the production of commodity chemicals.<sup>12,13</sup> This vision will shift the entire scope of the chemical industry from the prevailing petroleum refinery to LCB biorefinery.<sup>14,15</sup> LCB is usually available in the forms of crop residues, forest leftovers, waste paper etc.<sup>16</sup> The use of LCB as a feedstock for the biorefinery will reorient the global chemical industry and boost rural economy.<sup>17,18</sup>

LCB is primarily composed of cellulose (40–50%), hemicelluloses (20–40%), lignin (20–30%) and other trivial constituents such as protein, silica, and waxes.<sup>19,20</sup> Cellulose is a water-insoluble biopolymer derived from β-1,4 glycosidic bonds of anhydrous glucose units.<sup>21,22</sup> Irrespective of its robust structure, cellulose preferably needs to be depolymerized to glucose, which is in turn converted to platform biochemicals such as 5-hydroxymethylfurfural (HMF),<sup>23,24</sup> levuli-

<sup>a</sup>Key Laboratory for Industrial Biocatalysis, Ministry of Education of China, Institute of Applied Chemistry, Department of Chemical Engineering, Tsinghua University, Beijing 100084, China. E-mail: zhaoxb@mail.tsinghua.edu.cn, dhl Liu@tsinghua.edu.cn

<sup>b</sup>Department of Chemical Engineering, University of Gujarat, Gujarat 50700, Pakistan

nic acid,<sup>25,26</sup> lactic acid,<sup>27</sup> formic acid,<sup>2</sup> sorbitol,<sup>28</sup> bio-alcohols,<sup>29</sup> and biofuels.<sup>30,31</sup> Hemicelluloses are polysaccharides that are composed of various C5 and C6 monosaccharide units such as xylose, arabinose, mannose, glucose, etc.<sup>32,33</sup> Lignin is a conjugate complex polymer consisting of basic phenylpropane units including guaiacylpropane (G), syringylpropane (S), and 4-hydroxyphenylpropane (H).<sup>34,35</sup>

Polymeric materials such as polyethylene terephthalate, polyamides, and polyurethanes have played vital roles in the modern economy.<sup>36,37</sup> Several industries have started considering using bio-based chemicals to produce bioplastics.<sup>13,38</sup> Technically, bioplastics can be produced by different routes starting from LCB as described in Fig. 1. Of these routes, the chemical or biological conversion of LCB into monomers, fol-

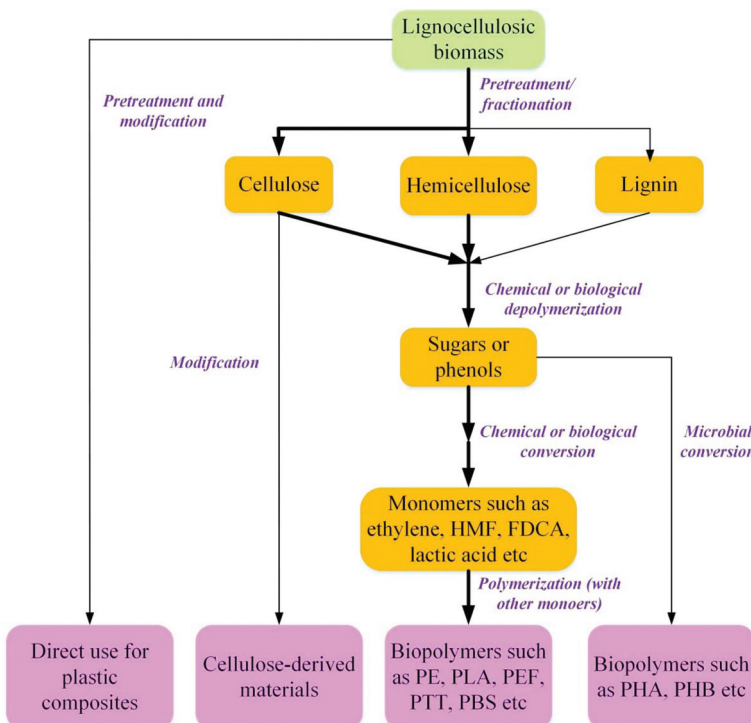


**Fig. 1** Typical production routes of bio-based polymers from lignocellulosic biomass.



Muhammad Sajid

*Mr. Muhammad Sajid is a Lecturer of Department of Chemical Engineering at University of Gujrat, Pakistan. He received his Bachelor degree and Master degree in Chemical Engineering at University of Punjab, Lahore, Pakistan in 2008 and 2012 respectively. He is now a PhD scholar at Institute of Applied Chemistry, Department of Chemical Engineering, Tsinghua University, China. His research interests include advanced catalytic process for the production of platform biochemicals from biomass-derived sugars.*



Xuebing Zhao

*Dr. Xuebing Zhao is an Associate Professor in Department of Chemical Engineering, Tsinghua University, China. He received his PhD degree in Department of Chemical Engineering at Tsinghua University in 2009, and performed his post-doctoral research work at Tsinghua University (2009–2011) and University of Wisconsin-Madison (2014–2015), respectively. His current research field include the biorefining of lignocellulosic biomass to produce biofuels and chemicals via chemical and biological approaches. He has published about 100 academic papers and book chapters. He was awarded Hou De-Bang Chemical Engineering Science and Technology Youth Award by the Chemical Industry and Engineering Society of China (CIESC) in the year of 2017.*

lowed by polymerization, is the most important way to produce bio-based polymers.<sup>39,40</sup> In a recent attempt, bioplastics have been successfully produced from bio-based ethylene glycol (EG) and furandicarboxylic acid (FDCA).<sup>41,42</sup> FDCA synthesis is considered as a precursor for the production of these green polymers, especially polyethylene 2,5-furandicarboxylate (PEF).<sup>43,44</sup> FDCA derived PEF is a real alternative to the fossil-based terephthalic acid (TPA) derived polyethylene terephthalate (PET).<sup>45,46</sup> PEF will not only serve as a novel replacement but will also improve salient features like excellent gas barrier performance, recyclability and extended mechanical properties.<sup>47</sup> Despite all the efforts and scientific research, the worldwide production of bioplastics is only a fraction of the total market supply.<sup>48,49</sup> Varieties of processes have been developed for the production of FDCA from biomass or biomass-derived sugars. There are generally four methods to produce FDCA:<sup>50,51</sup> (1) biological and chemical conversion of HMF; (2) catalytic transformation of numerous furan derivatives; (3) oxidation of 2,5 di-substituted furans; (4) dehydration of hexose derivatives. The objective of this work is to comprehensively review and discuss the catalytic conversion of HMF to produce FDCA, particularly focusing on the chemical-catalytic routes in terms of the process, kinetics and reaction mechanisms.

## FDCA as a chemical building block

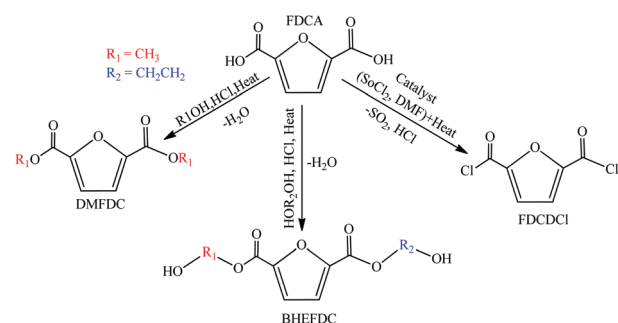
FDCA is one of the most important and promising candidates of the furan family due to its multi-functionality based on the cyclic structure and di-acidic side chains.<sup>52,53</sup> FDCA is found naturally in human urine<sup>54</sup> and blood plasma,<sup>55</sup> and has been utilized for the production of a variety of biochemicals such as succinic acid,<sup>16</sup> macrocyclic ligands,<sup>56</sup> fungicides,<sup>57</sup> isodecyl



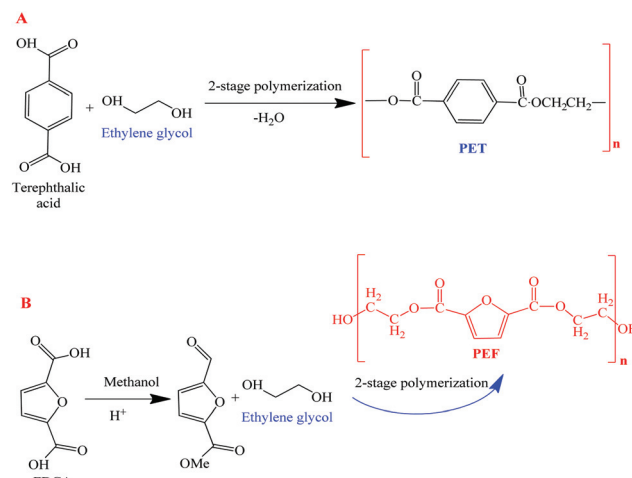
**Dehua Liu**

*Dr. Dehua Liu is a Professor and Director of Institute of Applied Chemistry, Department of Chemical Engineering, Tsinghua University, China. He received his PhD degree in Department of Chemical Engineering, Tsinghua University in 1991. His research field of interest includes production of biofuels and biochemicals from natural renewable biomass, especially focusing on biodiesel production from oil feedstock and microbial production of 1,3-propanediol from biodiesel by-product glycerol. He has published more than 250 academic papers. He has been awarded the First Award of the S&T Progress of China Petroleum and Chemical Industry Federation (CPCIF)(2006), "BlueSky Awards" for World's Leading Technology of Renewable Energy with Best Value of Investment (2016, 2018) and so on.*

furan-2,5-dicarboxylate,<sup>58</sup> isononyl furan-2,5-dicarboxylate,<sup>59</sup> dipentyl furan-2,5-dicarboxylate,<sup>60</sup> diheptyl furan-2,5-dicarboxylate,<sup>61</sup> thiolene films,<sup>62</sup> poly(ethylene dodecanedioate-2,5-furandicarboxylate) (PEDF),<sup>15</sup> 2-(1-oxopropoxy) and hexanedioic acid (PEA).<sup>63</sup> It is also applied as a corrosion inhibitor, pharmaceutical intermediate and crosslinking agent for polyvinyl alcohols.<sup>64</sup> The selective reduction of FDCA produces partially hydrogenated (2,5-dihydroxymethylfuran etc.), and fully hydrogenated (2,5-bis(hydroxymethyl) tetrahydrofuran) products that can be used as alcohol components in the production of new polyesters. A combination of these concepts to the production of new nylons, either through reactions of FDCA with diamines or through the conversion of FDCA to 2,5-bis(aminomethyl)tetrahydrofuran, could lead to future market bio-derivatives with multiple applications.<sup>65</sup> Hence, in view of the polymer process industry, FDCA is a highly demanding monomer because of its tremendous utilization in the production of different monomers like dichloride- (FDCDCl), dimethyl- (DMFDC), diethyl-, or bis(hydroxyethyl)- (BHEFDC) derivatives (Scheme 1),<sup>65</sup> for the production of polyesters, polyamides, and plasticizers. The carboxyl groups attached at the *para* positions of the furan rings are analogous to fossil-derived TPA,<sup>66</sup> and thus FDCA is an eco-friendly alternative for producing bioplastics.<sup>67</sup> Additionally, FDCA is also used for polyesters like polybutylene terephthalate (PBT) and polyethylene terephthalate (PET, Scheme 2),<sup>68</sup> which in turn are utilized in film and fiber production, packing materials and soft drink bottles.<sup>69,70</sup> Polyesters from FDCA are so appealing that just five years after the 1<sup>st</sup> FDCA patent, the Celanese Corporation of America (1946) filed a patent application for FDCA-derived PEF<sup>41</sup> followed by a patent by Mitsubishi for PEF and PBF synthesis.<sup>71</sup> PEF has excellent thermochemical properties with biodegradability that makes it a better choice in comparison to PET.<sup>46,72</sup> The synthesis of PEF has actually been investigated for more than 70 years<sup>73</sup> but its production has failed to conquer commercialization due to the relatively poor purity, process difficulties and sustainable availability of FDCA. The inclusion of FDCA in 12 platform biochemicals highlighted the extensive research for the sustainable commercial production of FDCA.<sup>11</sup> In 2011, Avantium revolutionized FDCA



**Scheme 1** FDCA derived monomers.<sup>65</sup>



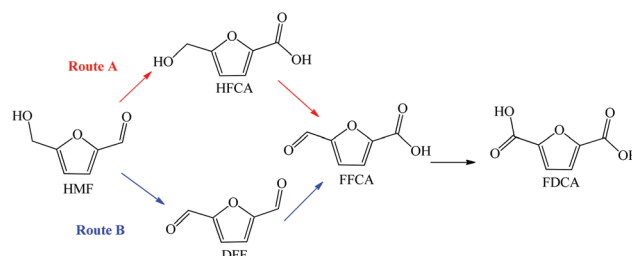
**Scheme 2** Comparison of the PEF and PET production processes. A: Production of PET from TPA; (B) production of PEF from FDCA.

production through the successful operation of its first pilot plant with production capacity of 40 tons per year;<sup>74</sup> this project unwrapped the industrialization of FDCA.

FDCA also has potential applications in medicine. The diethyl ester of FDCA has anesthetic properties similar to cocaine. Dicalcium 2,5-furandicarboxylate inhibits the growth of *Bacillus megatorum*.<sup>75</sup> FDCA-derived anilides demonstrate anti-bacterial actions and FDCA itself is a strong complexing agent; chelating with ions ( $\text{Ca}^{2+}$ ,  $\text{Cu}^{2+}$  and  $\text{Pb}^{2+}$ ) has increased its utilization in medicine for the removal of kidney stones.<sup>75</sup> Interestingly, HMF is metabolized *via* FDCA in mammals including humans. Manufacturing artificial veins for transplantation, *via* a dilute solution of FDCA in tetrahydrofuran, and many other medical utilizations are under investigation.

## Chemical oxidative production of 2,5-FDCA from HMF

HMF came out as a promising feedstock for the production of FDCA in the 19<sup>th</sup> century. Different reaction systems have been used for the oxidation of HMF with air, oxygen or other oxidizing agents ( $\text{H}_2\text{O}_2$ ,  $\text{KMnO}_4$  etc.).<sup>76</sup> Fig. 2 illustrates the diverse FDCA production processes from biomass and biomass-



**Scheme 3** Reaction pathway of HMF oxidation to produce FDCA.

derived intermediates. The chemical conversion requires high reaction conditions (temperature and pressure) and additives,<sup>77</sup> while biconversion proceeds *via* a mild process environment using biological catalysts.<sup>78</sup> The stepwise production of FDCA from biomass typically includes the following steps: (1) hydrolysis of lignocellulosic cellulose to glucose; (2) chemical and thermochemical conversion of glucose to platform biochemicals, *i.e.* dehydration of glucose to HMF; (3) catalytic-oxidation of HMF to FDCA. In this process, cellulose is usually firstly separated from hemicellulose and lignin by pretreatment, then converted to glucose by chemical or biological approaches, followed by isomerization of the obtained glucose to form fructose.<sup>79</sup> Direct utilization of glucose as feedstock proceeds *via* the *in situ* isomerization of glucose to fructose followed by dehydration to produce HMF, and oxidation of HMF further yields FDCA.

Depending on the system applied, the conversion of HMF to FDCA can proceed through the preferred aldehyde group oxidation to 5-hydroxymethyl-2-furan carboxylic acid (Scheme 3, route A), or the alcoholic group oxidation to 2,5-furan dicarboxaldehyde (Scheme 3, route B). These process intermediates are then oxidized to FFCA, which is in turn transformed into FDCA as the final product.<sup>80</sup>

## Historical methods

The production of FDCA was conducted as early as 1876 when Fittig *et al.* catalytically produced FDCA from mucic acid in 48% aqueous solution of hydrogen bromide (HBr) as indicated in Scheme 4.<sup>81</sup>

Mucic acid dehydration proceeds with different dehydrating agents for the efficient formation of FDCA. However, the mucic acid process failed to achieve scientific progress due to

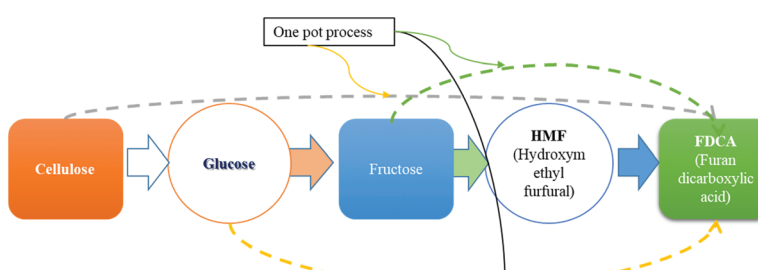
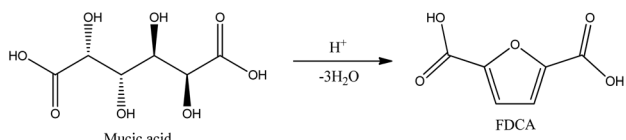
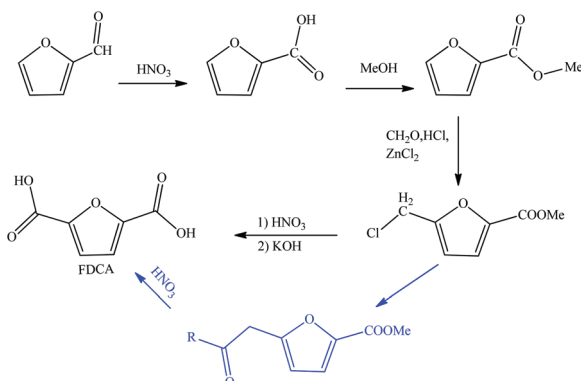


**Fig. 2** Schematic generalization of FDCA production processes from cellulose.



**Scheme 4** FDCA production through the dehydration of mucic acid.<sup>81</sup>



**Scheme 5** FDCA synthesis from furfural.<sup>83</sup>

its high cost, long reaction time (>20 hours) and relatively high reaction temperature (120 °C).<sup>82</sup> Following this, FDCA synthesis utilizing different starting materials in different mediums has been investigated.<sup>83</sup> Xylose-derived furfural could be an alternative raw material for FDCA production. In this process, inorganic oxidants (e.g. HNO<sub>3</sub>) can be initially used for furfural oxidation, followed by esterification of the formed 2-furoic acid with methanol to form an intermediate, which is finally converted to FDCA by several subsequent steps (Scheme 5).<sup>82,83</sup> As indicated by Scheme 5, the production of FDCA from furfural is complex with many intermediates, thus reducing the overall yield and selectivity, which has compelled researchers to search for alternative technologies for the efficient and economical production of FDCA. HMF oxidation to FDCA is advantageous because the oxidation process can be conducted with homogeneous catalysts,<sup>84</sup> heterogeneous catalysts,<sup>85</sup> biocatalysts,<sup>86</sup> or by electrochemical oxidation,<sup>87</sup> as well as without any catalyst,<sup>88</sup> or in an aqueous-organic biphasic system<sup>89</sup> that can facilitate the efficient separation of the product from the solution mixture.<sup>90</sup>

## **Homogenous catalytic methods**

Catalytic oxidation of HMF, either by a homogeneous or heterogeneous catalyst, is still the most promising and extensively researched FDCA production pathway. However, the utilization of homogeneous catalysts is less attractive as compared to heterogeneous catalysts, due to the separation and recycling problems.<sup>88</sup> High-pressure air oxidation of HMF with Co(OAc)<sub>2</sub>, Mn(OAc)<sub>2</sub>, and HBr could produce FDCA with a yield of 60.9%. Using Co(OAc)<sub>2</sub>/Zn(OAc)<sub>2</sub>/NaBr can only produce DFF, and the addition of trifluoroacetic acid can promote the FDCA production (60% yield).<sup>91</sup> Pure oxygen and *t*-BuOOH have been

applied as oxidants. *t*-BuOOH with only CuCl<sub>2</sub> resulted in an FDCA yield of 45% and the addition of LiBr to this system reduced the yield to 43%.<sup>91</sup>

The practical utilization of homogeneous catalysts in the oxidative production of FDCA from HMF mainly suffers from two discrete drawbacks, *i.e.* lower FDCA yield and the formation of byproducts.<sup>88</sup> The separation of the catalysts and purification of the product are also major hurdles along with recycling deficiencies. In contrast, heterogeneous catalysis demonstrates several merits, with the facile separation and recycling due to the heterogeneous nature.<sup>92</sup> Therefore, heterogeneous catalysis has attracted more interest for practical application and potential commercialization as compared to homogeneous catalysis.

### Heterogeneous catalytic methods

The oxidative production of FDCA from HMF over different heterogeneous catalysts has been studied extensively in various process environments. Mostly, the oxidation proceeds with either pure oxygen or air as an oxidizing agent; hydrogen peroxide ( $H_2O_2$ ) and potassium permanganate ( $KMnO_4$ ) have also been used but researchers mostly prefer molecular oxygen considering its higher oxidation potential, eco-friendly impact and low cost. Different metal supported heterogeneous catalysts, such as platinum (Pt), gold (Au), ruthenium (Ru) and palladium (Pd), with good catalytic activity, recyclability and stability, have also been developed and successfully applied in HMF oxidation to FDCA.<sup>88</sup> Noble metal oxides occupy the major portion of the heterogeneous catalysis scheme in the current FDCA research regime.

#### HMF oxidation to FDCA over Pt supported catalysts.

Supported platinum (Pt) catalysts are dynamic for the aerobic oxidation of HMF as compared to other noble metal catalysts.<sup>88</sup> When applied to HMF oxidation, carbon supported Pt catalysts (Pt/C and Pt–Pb/C) can give 81% yield of FDCA with lead (Pb)-free Pt/C and 99% with Pt–Pb/C catalyst under 1 bar O<sub>2</sub> pressure (Table 1).<sup>93</sup> The detection of HFCA as an intermediate proves the preferred oxidation of the formyl group over the hydroxymethyl group with the lead-doped Pt catalyst (Scheme 3, route A). Yield increment with Pb-doping stimulated the development of bimetallic catalysts for HMF oxidation. Following this, the bismuth (Bi)-incorporated Pt catalyst (Pt–Bi/C) having a Pt–Bi molar ratio of 0.2 was developed and applied in FDCA synthesis.<sup>94</sup> A 29% increase in FDCA yield by Bi addition proved the improvement in the activity of the bimetallic catalyst with identical parameters.<sup>95</sup> Pressure reduction negatively affected the yield and an increase in pressure did not exhibit appreciable effects (Table 1).<sup>96</sup> As such, 1 bar oxygen pressure is the optimum pressure for the Pt/C catalyst that is easy to maintain without any potential hazard. The rapid oxidation of process intermediates, HFCA and DFF, produces FFCA. FFCA oxidation to FDCA is the rate-controlling step. Bi incorporation to produce Pt–Bi/C catalyst can exceptionally stabilize the catalyst by eliminating the oxygen poisoning and Pt leaching tendency, resulting in increased catalyst life and stability.

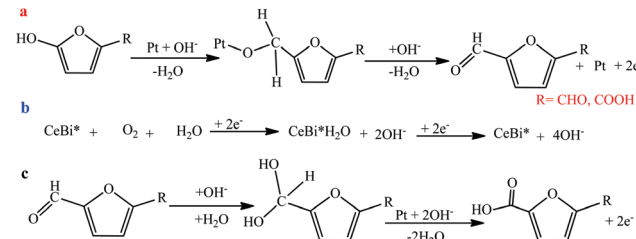
**Table 1** Some recently reported works on the oxidation of HMF for the production of FDCA over Pt supported catalysts

Catalyst	Base	Oxidant	Time (h)	T (°C)	FDCA yield (%)	HMF con. (%)	Ref.
Pt-Pb/C	1.25 M NaOH	1 Bar O <sub>2</sub>	2	25	99	100	93
Pt/C	1.25 M NaOH	1 Bar O <sub>2</sub>	2	25	81	100	93
Pt-Bi/C	2 equiv. Na <sub>2</sub> CO <sub>3</sub>	40 Bar air	6	100	>99	100	94
Pt/C	2 equiv. Na <sub>2</sub> CO <sub>3</sub>	40 Bar air	6	100	69	99	94
Pt-Bi/TiO <sub>2</sub>	2 equiv. Na <sub>2</sub> CO <sub>3</sub>	40 Bar air	6	100	99	>99	97
Pt/TiO <sub>2</sub>	2 equiv. Na <sub>2</sub> CO <sub>3</sub>	40 Bar air	6	100	84	90	97
Pt/RGO	5 equiv. NaOH	1.01325 Bar O <sub>2</sub>	24	25	84	100	98
Pt/C	2 equiv. NaOH	6.90 Bar O <sub>2</sub>	6	22	79	100	95
Pt/C	pH = 13	10 Bar O <sub>2</sub>	4	50	80	100	96
Pt/Al <sub>2</sub> O <sub>3</sub>	pH = 9	0.2 Bar O <sub>2</sub>	6	60	99	100	99
Pt/Al <sub>2</sub> O <sub>3</sub>	1 equiv. Na <sub>2</sub> CO <sub>3</sub>	1 Bar O <sub>2</sub>	12	75	96	96	100
Pt/ZrO <sub>2</sub>	1 equiv. Na <sub>2</sub> CO <sub>3</sub>	1 Bar O <sub>2</sub>	12	75	94	100	100
Pt/ZrO <sub>2</sub>	Base free	4 Bar O <sub>2</sub>	12	100	97.3	100	101
Pt/C	1 equiv. Na <sub>2</sub> CO <sub>3</sub>	1 Bar O <sub>2</sub>	12	75	89	100	100
Pt/TiO <sub>2</sub>	1 equiv. Na <sub>2</sub> CO <sub>3</sub>	1 Bar O <sub>2</sub>	12	75	2	96	100
Pt/CeO <sub>2</sub>	1 equiv. Na <sub>2</sub> CO <sub>3</sub>	1 Bar O <sub>2</sub>	12	75	8	100	100
Pt/Ce <sub>0.8</sub> Bi <sub>0.2</sub> O <sub>2-δ</sub>	4 equiv. NaOH	10 Bar O <sub>2</sub>	0.5	23	98	100	102
Pt/CeO <sub>2</sub>	4 equiv. NaOH	10 Bar O <sub>2</sub>	0.5	23	20	100	102
Pt/PVP	Base free	1 Bar O <sub>2</sub>	24	80	94	100	103
Pt/IP	Base free	1 Bar O <sub>2</sub>	24	80	99	100	103
Fe <sub>3</sub> O <sub>4</sub> @C/Pt	1.67 equiv. Na <sub>2</sub> CO <sub>3</sub>	1 Bar O <sub>2</sub>	4	90	84	100	104
Pt-NP5	Base free	1 Bar O <sub>2</sub>	6	80	60	100	105
Pt-NP-Cl	Base free	1 Bar O <sub>2</sub>	6	80	65	100	105

The effects of the supports have been investigated by producing Pt-Bi/TiO<sub>2</sub> and Pt/TiO<sub>2</sub> catalysts and replacing the C support with TiO<sub>2</sub>. The TiO<sub>2</sub> effectively and selectively increased the FDCA yield (Table 1). Reduced graphene oxides (RGOs) with their abundant surface functional groups are also promising catalyst supports and are now being applied extensively. When the support was changed to RGO (Pt/RGO), quantitative FDCA yield was observed (84%) in 24 hours but the RGO support did not work efficiently with other noble metal catalysts such as Pd/RGO, Rh/RGO and Ru/RGO. This demonstrates the catalytic superiority of Pt over other noble metals (Table 1).<sup>98</sup> However, an increase in the process intermediate (HFCA) and a decrease in the final product (FDCA) was observed during the recycling experiments.

The substantial aim of low-pressure oxidation can be achieved by applying relatively cheap metal oxide-supported Pt catalysts. Exceptionally high yield (>99%) was recorded with very low oxygen pressure (0.2 bar) in alkaline medium.<sup>99,106</sup> Oxygen chemisorption on the active sites of the Pt/γ-Al<sub>2</sub>O<sub>3</sub> catalyst negatively affected and deactivated the catalytic ability.<sup>100</sup> Changing the metal oxide support resolved the problem of catalyst deactivation. Pt/ZrO<sub>2</sub>, Pt/C and Pt/γ-Al<sub>2</sub>O<sub>3</sub> all performed well and Pt/TiO<sub>2</sub> and Pt/CeO<sub>2</sub> showed poor catalytic efficiency under similar conditions (Table 1).<sup>100</sup> Bi-Added bimetallic catalyst could improve the yield to 98% over Pt/Ce<sub>0.8</sub>Bi<sub>0.2</sub>O<sub>2-δ</sub> (Table 1).<sup>102</sup> These results suggest that non-reducible oxide (γ-Al<sub>2</sub>O<sub>3</sub>, ZrO<sub>2</sub>, and C)-supported Pt catalysts have higher catalytic performance than reducible oxide (TiO<sub>2</sub> and CeO<sub>2</sub>)-supported Pt catalysts due to the low oxygen storage capacity.

Reaction kinetics have shown that HMF oxidation proceeds through the Pt-alkoxide intermediate.<sup>102</sup> Pt-Nanoparticles yield Pt-alkoxides by reacting with the hydroxyl groups present in

**Scheme 6** The proposed HMF oxidation mechanism in aqueous alkaline solution; CeBi\* denotes oxygen opening accompanied by Bi.<sup>102</sup>

HMF, substituting β-H with hydroxide ions (OH<sup>-</sup>). Bi-Containing ceria accelerates the oxygen reduction due to the availability of more oxygen vacancies and the breakup of transitional peroxides (Scheme 6).<sup>102</sup> This smooth catalytic cycle continues to consume surface electrons in oxygen reduction, which safeguards the catalytic efficiency and the Pt/Ce<sub>0.8</sub>Bi<sub>0.2</sub>O<sub>2-δ</sub> catalyst can work efficiently even in the fifth cycle. It has been reported that the observed yield of FDCA was 97% in the fifth cycle, which was appreciably close to the recorded yield in the first batch (98%).<sup>102</sup>

Alkaline medium oxidation of HMF is kinetically favorable and gives higher FDCA yield but the separation of inorganic salt and neutralization of the product solution are major problems.<sup>107</sup> To overcome this, base-free oxidation has been investigated.<sup>103</sup> The observed yield can be high enough (95%) over PVP-stabilized Pt nanoparticles (Pt/PVP) with low oxygen pressure, but long reaction time (24 hours), low feed rate (0.29 m mole), and high catalyst loading (5 moles%) are the major disadvantages of this system.<sup>103</sup> Hence, at this stage, the Pt/PVP catalyst is uneconomical for mass production although it has high stability and recyclability with confirmation of the

green environment protocol. Platinum nanoparticles (Pt-NPs) dispersed in water have been widely employed as oxidation catalysts due to their strong oxidizing ability and diverse stability.<sup>108</sup> Pt-NPs-doped polymeric catalysts can not only stabilize the Pt-NPs by steric and electrosteric interactions but also boost the catalytic activity. Among the different counteranions explored so far, the Tf<sub>2</sub>N<sup>-</sup> anion has exhibited the highest catalytic activity, presumably because it may be displaced from the NP surface in a facile manner, generating catalytically active surface sites where the substrates can bind and react, while simultaneously offering sufficient electronic and steric protection to stabilize the NPs during reaction.<sup>105</sup>

**HMF oxidation to FDCA over Pd supported catalysts.** Palladium (Pd) promotes HMF oxidation in a similar manner to Pt but the FDCA yield is relatively low in comparative combinations.<sup>95</sup> Numerous Pd catalysts have been developed by doping palladium nanoparticles (Pd-NPs) with C, PVP and metal oxides as support materials. Stabilized Pd (Pd/PVP) catalyst gives a quantitative yield as with Pt.<sup>103,109</sup> Pd-NPs size can be controlled by alkali dosing (NaOH) during the alcoholic preparation of the Pd/PVP catalyst. The size of Pd-NPs in the catalyst cluster inversely affects the FDCA yield. Reduced FDCA yield (81%) was observed when particle diameter increased from 1.8 nm to 2 nm as shown in Table 2.<sup>109</sup> The increased amount of surface atoms and unsaturated active metal sites have been recognized as a possible reason for the increased reactivity of Pd/PVP nanoparticles with reduced particle size. Interestingly, oxygen flow rate also affects the catalytic activity; hence, precise control of the optimum flow rate is highly recommended for economical yield. Oxygen chemisorption due to excessive availability might cause deactivation of the catalyst.<sup>88</sup> At low reaction temperature (<70 °C), the rate of reaction from FFCA to FDCA is higher than the rate of HFCA to FFCA and the products exhibit a maximum HFCA, whereas at a higher temperature (>90 °C) both oxidation rates are nearly equal and the key product will be exclusively FDCA.<sup>109</sup> In alkaline medium, the Pd/PVP catalyst suffers from recycling and stability problems, but the stability can be improved by metal oxide impregnation. Assimilation of different metal-oxides such as TiO<sub>2</sub>, γ-Al<sub>2</sub>O<sub>3</sub>, KF/Al<sub>2</sub>O<sub>3</sub>, and ZrO<sub>2</sub>/La<sub>2</sub>O<sub>3</sub> usually expands the efficiency of the catalysts. Pd metal oxide combi-

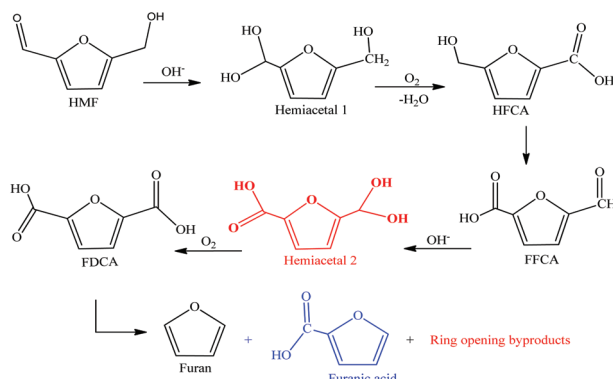
nation in Pd/ZrO<sub>2</sub>/La<sub>2</sub>O<sub>3</sub> catalyst increases the yield (90%) and stability over other oxides (Table 2).<sup>110</sup> There is rare Pd-NPs aggregation in contrast to other catalysts (Pd-metal oxide) as analyzed by TEM. Separation and recycling using external magnetic can be further improved by introducing magnetized Pd catalysts.<sup>111,112</sup> Similarly, bimetallic catalyst (Pd-Au/HT) results in higher yield and stability in recycling experiments without reducing its reactivity.<sup>113</sup>

A magnetized Pd catalyst ( $\gamma$ -Fe<sub>2</sub>O<sub>3</sub>@HAP-Pd) has been developed by coating hydroxyapatite [HAP = Ca<sub>10</sub>(PO<sub>4</sub>)<sub>6</sub>(OH)<sub>2</sub>] on  $\gamma$ -Fe<sub>2</sub>O<sub>3</sub> and Pd<sup>2+</sup> was replaced by the Ca<sup>2+</sup> in the HAP macromolecule and was then reduced to Pd<sup>(0)</sup>-NPs.<sup>77</sup> The catalyst showed higher FDCA yield with complete HMF conversion (Table 2). Magnetism eases the separation of heterogeneous catalyst from the reaction mixture with the help of an external magnet, increasing the recyclability without reducing catalytic activity.<sup>77</sup> Recently developed graphene oxides (GO) are successfully replacing carbon as a catalyst supporting material because both retain higher surface area with oxygen functional groups. Separation and recycling difficulties of C-based nanoparticles can be easily overcome by replacing them with graphene oxide supported NPs and magnetized catalysts. A magnetically separable catalyst (C-Fe<sub>3</sub>O<sub>4</sub>-Pd) prepared using a one-step solvothermal process by simultaneously doping Pd and Fe<sub>3</sub>O<sub>4</sub> nanoparticles demonstrated an upgraded product yield (91.8%) under mild process parameters (Table 2).<sup>111</sup> A carbon-supported magnetic catalyst (Pd/C@Fe<sub>3</sub>O<sub>4</sub>), prepared by *in situ* glucose carbonization on Fe<sub>3</sub>O<sub>4</sub> microspheres, provided high yield and cyclic stability.<sup>112</sup> Low alkali requirements, atmospheric pressure (oxygen), ease of separation and recycling, good recycling efficiency and constant reactivity are the profound advantages associated with the use of heterogeneous magnetic Pd catalysts.

**HMF oxidation to FDCA over Au supported catalysts.** Initially, gold (Au) was considered inactive as a catalyst for chemical transformations till the 1980s and the discovery of its catalytic ability was a stunning breakthrough for research and development.<sup>117,118</sup> Recently, many Au catalysts were developed and applied successfully for a wide range of potential applications.<sup>119,120</sup> Au catalysts display encouraging performance for HMF oxidation and their catalytic efficiency is strongly

**Table 2** Some recently reported works on the oxidative production of FDCA from HMF over Pd supported catalysts

Catalyst	Base	Oxidant	Time (h)	T (°C)	FDCA yield (%)	HMF con. (%)	Ref.
Pd/C	2 equiv. NaOH	6.9 Bar O <sub>2</sub>	6	23	71	100	95
Pd/PVP	1.25 equiv. NaOH	1.01325 Bar O <sub>2</sub>	6	90	90	>99	109
Pd/ZrO <sub>2</sub> /La <sub>2</sub> O <sub>3</sub>	1.25 equiv. NaOH	1.01325 Bar O <sub>2</sub>	6	90	90	>99	110
Pd/Al <sub>2</sub> O <sub>3</sub>	1.25 equiv. NaOH	1.01325 Bar O <sub>2</sub>	6	90	78	>99	110
Pd/Ti <sub>2</sub> O <sub>3</sub>	1.25 equiv. NaOH	1.01325 Bar O <sub>2</sub>	6	90	53	>99	110
$\gamma$ -Fe <sub>2</sub> O <sub>3</sub> @HAP-PD	0.5 equiv. K <sub>2</sub> CO <sub>3</sub>	1.01325 Bar O <sub>2</sub>	6	100	92.9	97	77
C-Fe <sub>3</sub> O <sub>4</sub> -Pd	0.5 equiv. K <sub>2</sub> CO <sub>3</sub>	1.01325 Bar O <sub>2</sub>	4	80	91.8	98.1	111
Pd/C@Fe <sub>3</sub> O <sub>4</sub>	0.5 equiv. K <sub>2</sub> CO <sub>3</sub>	1.01325 Bar O <sub>2</sub>	6	80	86.7	98.4	112
Pd/TiO <sub>2</sub>	2 equiv. NaOH	10 Bar O <sub>2</sub>	4	90	9	100	114
Pd/HT	Base free	1 Bar O <sub>2</sub>	7	100	>99	>99	115
Pd/CC	0.5 equiv. K <sub>2</sub> CO <sub>3</sub>	O <sub>2</sub> @20 ml min <sup>-1</sup>	30	140	85	100	116
Pd-Au/HT	2 equiv. NaOH	O <sub>2</sub> @60 ml min <sup>-1</sup>	6	60	90	100	113



**Scheme 7** Aerobic oxidation reaction mechanisms for aqueous HMF over the Au/CeO<sub>2</sub> catalyst.<sup>121</sup>

influenced by supporting materials, being similar to other noble metal (Pt and Pd) catalysts.<sup>121</sup> Metal oxide supports play a vibrant role and gold nanoparticles (Au-NPs) doped on CeO<sub>2</sub> and TiO<sub>2</sub> could obtain higher FDCA yield (>99%) than Fe<sub>2</sub>O<sub>3</sub> and C.<sup>122</sup> Although the yield is superior (96%) over the Au/CeO<sub>2</sub> catalyst as compared to the Au/TiO<sub>2</sub> catalyst with higher HMF/Au ratio (640), the high oxygen pressure and activity reduction in the recycling experiments are paramount industrial barriers.<sup>121</sup> The reactions proceed with HFCA and hemiacetal intermediates following the same route as illustrated in Scheme 7.

The catalytic activity of Au/CeO<sub>2</sub> can be further improved by Bi<sup>3+</sup> incorporation into the CeO<sub>2</sub> support nanostructure.<sup>123</sup> The modified catalyst not only expands O<sub>2</sub> activation but also increases the hydride transferability of nano-CeO<sub>2</sub>, due to the availability of lone pair electrons (Bi<sup>3+</sup>). The Bi combined catalyst, [Au/Ce<sub>1-x</sub>Bi<sub>x</sub>O<sub>2-δ</sub>] (0.08 ≤ x ≤ 0.5)], can increase the FDCA yield to 75% from 39% over unaided Au/CeO<sub>2</sub> under the same

conditions.<sup>121,123</sup> Increased FDCA yield was observed with an increase in reaction time over Au/Ce<sub>0.9</sub>Bi<sub>0.1</sub>O<sub>2-δ</sub> catalyst (Table 3).<sup>123</sup> The catalyst can be easily separated and recycled with an acceptable decrease in catalytic activity. The catalytic support dependency of Au catalysts has also been investigated by developing HY-zeolite catalysts.<sup>124</sup> The FDCA yield in alkaline medium is selectively high (>99%) over the Au/HY catalyst in comparison to channel-type zeolites (ZSM-5 & H-MOR), TiO<sub>2</sub>, Mg(OH)<sub>2</sub> and CeO<sub>2</sub> catalysts (Table 3).<sup>124</sup> The efficiency enrichment is due to the uniform dispersion of Au nanoclusters in the HY zeolite super-cage structure. The developed cage structure eradicates the NP agglomeration, which thus increases the recycling efficiency and performance of the catalyst.<sup>125</sup> The addition of 1,3 propanediol further improves the process efficiency by suppressing the self-polymerization and humin formation over Au metal oxide catalysts.<sup>126</sup>

Numerous bimetallic Au catalysts with extended physicochemical properties were prepared and tested for the aerobic oxidation of HMF. These bimetallic catalysts further improved the process efficiency and catalyst stability.<sup>127</sup> The physicochemical properties of the developed catalyst can be altered by composition, extent and equality of mixing.<sup>127,128</sup> The Au–Cu/TiO<sub>2</sub> (bimetallic) catalyst is very stable and more efficient than the Au/TiO<sub>2</sub> catalyst due to strong synergistic effects.<sup>129</sup> It not only eliminates the PVP-stabilized Au post-deposition but also accelerates the FDCA yield, reducing competitive reactions. It also improves the efficient recycling without significant agglomeration and leaching of metallic nanoparticles in the catalyst arrangement. Similar findings have also been recorded with Au–Cu/CeO<sub>2</sub>, Au–Cu/TiO<sub>2</sub> and Au–Pd/AC catalysts (Table 3).<sup>123,130,131</sup> Au–Pd/AC is stable but with decreased recycling efficiency. Extraordinarily superior stability and yield were observed (99% in the fifth cycle) when the modified Au<sub>8</sub>–Pd<sub>2</sub>/AC catalyst was applied.<sup>131</sup> Hence, the deactivation of monometallic Au catalysts by the adsorption of reaction inter-

**Table 3** Oxidative production of FDCA from HMF over Au support catalysts

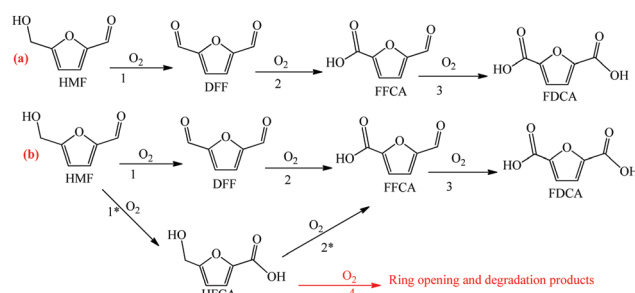
Catalyst	Base	Oxygen pressure	Time (h)	T (°C)	FDCA yield (%)	HMF conc. (%)	Ref.
Au/C	2 equiv. NaOH	6.9 Bar O <sub>2</sub>	6	23	7	100	95
Au/CeO <sub>2</sub>	2 equiv. NaOH	10 Bar air	5	130	96	100	121
Au/TiO <sub>2</sub>	4 equiv. NaOH	10 Bar air	8	130	84	100	121
Au/Ce <sub>0.9</sub> Bi <sub>0.1</sub> O <sub>2-δ</sub>	5 equiv. NaOH	1 Bar O <sub>2</sub>	2	65	>99	100	123
Au/HY	5 equiv. NaOH	0.3 Bar O <sub>2</sub>	6	60	>99	>99	124
Au/CeO <sub>2</sub>	5 equiv. NaOH	0.3 Bar O <sub>2</sub>	6	60	73	>99	124
Au/TiO <sub>2</sub>	5 equiv. NaOH	0.3 Bar O <sub>2</sub>	6	60	85	>99	124
Au/Mg(OH) <sub>2</sub>	5 equiv. NaOH	0.3 Bar O <sub>2</sub>	6	60	76	>99	124
Au/H-MOR	5 equiv. NaOH	0.3 Bar O <sub>2</sub>	6	60	15	96	124
Au/Na-ZSM5-25	5 equiv. NaOH	0.3 Bar O <sub>2</sub>	6	60	1	92	124
Au/TiO <sub>2</sub>	20 equiv. NaOH	20 Bar O <sub>2</sub>	18	30	71	100	125
Au/TiO <sub>2</sub>	pH = 13	10 Bar O <sub>2</sub>	4	50	80	100	96
Au–Cu/TiO <sub>2</sub>	4 equiv. NaOH	10 Bar O <sub>2</sub>	4	95	99	100	129
Au <sub>8</sub> –Pd <sub>2</sub> /C	2 equiv. NaOH	30 Bar O <sub>2</sub>	2	60	>99	>99	131
Au/HT	Base-free	1 Bar O <sub>2</sub>	7	95	>99	>99	133
Au–Pd/CNT	Base-free	5 Bar O <sub>2</sub>	12	100	94	100	132
Au–Pd/CNT	Base-free	10 Bar air	12	100	96	100	132
Au/TiO <sub>2</sub>	4 equiv. NaOH	10 Bar O <sub>2</sub>	4	70	19	100	114
Au/m-CeO <sub>2</sub>	4 equiv. NaOH	10 Bar O <sub>2</sub>	4	70	92	100	135
Au/CeO <sub>2</sub>	0.2 equiv. Na <sub>2</sub> CO <sub>3</sub>	5 Bar O <sub>2</sub>	15	140	91	>99	126

mediates as compared to bimetallic catalysts verifies that bimetallic Au catalysts are superior in activity and stability.

Environmental concerns associated with the use of alkaline solution, salt separation, recycling and product solution neutralization can be addressed by employing base-free HMF oxidation over a hydrotalcite-supported (Au/HT) catalyst.<sup>133</sup> The elimination of the acid requirement for product solution neutralization caused the base-free process to be more cost competitive and selective as compared to other alkaline medium oxidation processes. Some reported base-free processes can be performed with high FDCA yield (99%) and complete HMF conversion under low oxygen pressure (Table 3). Au/MgO, Au/Al<sub>2</sub>O<sub>3</sub>, Au/SiO<sub>2</sub> and Au/C either remain unreactive or exhibit very low reactivity, whereas Au/HT unveils exceptional catalytic activity in a base-free environment; however, the recycling performance decreases.<sup>133</sup> Mg<sup>2+</sup> leaching from the HT support was observed due to the HT-FDCA chemical interaction, which limits the base-free conditions.<sup>134</sup> The development of carbon nanotubes (CNT) supported Au-Pd catalyst (CNT-Au-Pd) revolutionarily accelerated the base-free FDCA production.<sup>132</sup> The CNT-Au-Pd catalyst is more efficient when oxygen is replaced

with air under moderately high pressure (Table 3).<sup>132</sup> The CNT supported reactant adsorption with improved exposed sites and strong synergistic Au-Pd effects can contribute efficiently to the catalyst performance. Evidence of FFCA and DFF as reaction intermediates indicate the preferred oxidation of the hydroxyl group, as compared to the aldehyde group, using the Au-Pd/CNT catalyst [Scheme 8(a)].<sup>132</sup> The monometallic Au/CNT catalyst, as compared with the bimetallic Au-Pd/CNT catalyst, preferentially oxidizes the aldehyde group, producing the HFCA intermediate and conforming to the same processing scheme as over Au/CeO<sub>2</sub> and Au/TiO<sub>2</sub> catalysts in an alkaline environment.<sup>121</sup> Unfortunately, HFCA initiates competitive reactions by furan ring opening and degradation [Scheme 8(b)].<sup>132</sup> The monometallic Pd/CNT and bimetallic Au-Pd/CNT catalysts propagate the reaction through identical pathways. However, Pd addition in the Au-CNT structure modifies the reaction pathway to DFF from HFCA conversion and accelerates the FFCA to FDCA oxidation.

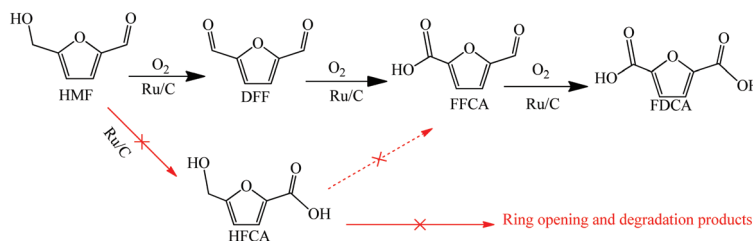
**HMF oxidation to FDCA over Ru supported catalysts.** Being similar to Pt, Ruthenium (Ru)-based catalysts can also be used to catalyze the oxidation of HMF.<sup>136</sup> Initially, Ru based catalysts were mostly applied to the oxidation of HMF to DFF rather than to FDCA production.<sup>137–139</sup> The mechanism of oxidation, the potential of Ru-oxide catalysts [Ru(OH)<sub>x</sub>] and the effects of the base material (La<sub>2</sub>O<sub>3</sub>, MgO, and HT) have already been discussed in detail.<sup>140,141</sup> Keeping in mind the performance of the C-support (as Pd/C and Au/C) in alkaline medium, the Ru/C catalyst was developed and applied in the HMF oxidation to FDCA. The practical FDCA yield is terribly low even at high oxygen pressure (Table 4).<sup>96</sup> An increasing trend was observed by using different bases and the highest yield was obtained with CaCO<sub>3</sub>.<sup>142</sup> Strong alkali (NaOH) not only affords lower yields but also degrades the HMF. This phenomenon indicates the instability of HMF at higher pH and suggests the use of weak bases. On the other hand, FDCA was recovered as



**Scheme 8** Reaction path for the aerobic oxidation of HMF to FDCA: (a) Pd/CNT and Au-Pd/CNT catalysts, (b) Au/CNT catalyst.<sup>132</sup>

**Table 4** Recent reported works on the oxidative production of FDCA from HMF over Ru supported catalysts

Catalyst	Base	Oxygen pressure	Time (h)	T (°C)	FDCA yield (%)	HMF conv. (%)	Ref.
Ru/C	pH = 13	10 Bar O <sub>2</sub>	4	50	6.48	98.05	96
Ru/C	1 equiv. NaOH	2 Bar O <sub>2</sub>	5	120	69	100	142
Ru/C	1 equiv. K <sub>2</sub> CO <sub>3</sub>	2 Bar O <sub>2</sub>	5	120	80	100	142
Ru/C	1 equiv. Na <sub>2</sub> CO <sub>3</sub>	2 Bar O <sub>2</sub>	5	120	93	100	142
Ru/C	1 equiv. HT	2 Bar O <sub>2</sub>	5	120	90	100	142
Ru/C	1 equiv. CaCO <sub>3</sub>	2 Bar O <sub>2</sub>	5	120	95	100	142
Ru/C	Base free	2 Bar O <sub>2</sub>	10	120	88	100	142
Ru(OH) <sub>x</sub> /MgO	Base free	2.5 Bar O <sub>2</sub>	20	140	96	100	143
Ru(OH) <sub>x</sub> /MgAl <sub>2</sub> O <sub>4</sub>	Base free	2.5 Bar O <sub>2</sub>	42	140	60	100	143
Ru(OH) <sub>x</sub> /HT	Base free	2.5 Bar O <sub>2</sub>	6	140	100	100	143
Ru(OH) <sub>x</sub> /HT	Base free	1 Bar O <sub>2</sub>	38	140	>98	100	143
Ru/MnCo <sub>2</sub> O <sub>4</sub>	Base free	24 Bar air	10	120	99.1	100	144
Ru/CoMn <sub>2</sub> O <sub>4</sub>	Base free	24 Bar air	10	120	82.2	100	144
Ru/MnCo <sub>2</sub> CO <sub>3</sub>	Base free	24 Bar air	10	120	69.9	99.9	144
Ru/ZrO <sub>2</sub>	Base free	10 Bar O <sub>2</sub>	16	120	71	100	145
Ru/AC	1 equiv. Na <sub>2</sub> CO <sub>3</sub>	35% H <sub>2</sub> O <sub>2</sub>	6	75	91.3	100	89
Ru/AC	4 equiv. NaHCO <sub>3</sub>	40 Bar air	2	100	75	100	148
Ru/AC-NaOCl	4 Equiv. NaHCO <sub>3</sub>	40 Bar air	4	100	55	100	148
Ru/HAP	Base free	10 Bar O <sub>2</sub>	24	120	99.6	100	146
Ru/HAP	Base free	10 Bar O <sub>2</sub>	24	140	99.9	100	146



Scheme 9 The reaction mechanism for FDCA production from HMF over Ru/C catalyst.<sup>142</sup>

its calcium salt because of the presence of unreacted calcium carbonate for the lower dissolution rate of CaCO<sub>3</sub>,<sup>142</sup> which acts as a neutralizer rather than a promoter of oxidation. This difficulty compels researchers to use base-free oxidation over Ru/C catalyst. Astonishingly, the quantitative FDCA yield (88%) was observed as a white precipitate, indicating a pure product without any competitive soluble byproduct. The Ru/C catalyst is highly stable in recycling experiments with just a slight decrease in catalytic activity, which is easy to regenerate by H<sub>2</sub>/Ar. FDCA production proceeds through the DFF route over Ru/C catalyst (Scheme 9). Process intermediates, DFF and FFCA can be well oxidized to FDCA over the Ru/C catalyst.<sup>142</sup>

HMF oxidation to produce FDCA was also investigated by employing diverse combinations of Ru-metal oxides catalysts in ionic liquids (ILs).<sup>143</sup> Ru(OH)<sub>x</sub>/HT gives the highest yield in a base-free environment with 100% conversion of HMF (Table 4).<sup>143</sup> Nevertheless, despite all the efforts, ILs were unsuccessful for use in large-scale FDCA production because of the high cost, relatively low FDCA yield (48%), inefficient separation from the product mixture and unsatisfactory catalytic stability.<sup>88</sup> These problems shifted the reaction medium to base-free aqueous phase oxidation over MnCo<sub>2</sub>O<sub>4</sub> supported Ru catalyst.<sup>144</sup> An exceptionally high yield of FDCA (99.1%) was reported under moderate conditions with very small impurities of FFCA (5-formylfuran-2-carboxylic acid) (Table 4).<sup>144</sup> The active sites of Brønsted and Lewis acids on the catalyst (Ru/MnCo<sub>2</sub>O<sub>4</sub>) surface can increase the yield. Supporting material (MnCo<sub>2</sub>O<sub>4</sub>) present in the catalyst structure plays a significant role and promotes HMF oxidation. Replacing this material (MnCo<sub>2</sub>O<sub>4</sub>) with CoMn<sub>2</sub>O<sub>4</sub> adversely affects the FDCA yield and reduces the conversion of FFCA to FDCA. The system performance was found to be affected by the distorted spinel structures of the CoMn<sub>2</sub>O<sub>4</sub> body-centered tetragonal crystalline structure in comparison to the cubic structure of MnCo<sub>2</sub>O<sub>4</sub>, with low surface area (CoMn<sub>2</sub>O<sub>4</sub> = 89.5 m<sup>2</sup> g<sup>-1</sup> vs. MnCo<sub>2</sub>O<sub>4</sub> = 151 m<sup>2</sup> g<sup>-1</sup>) and low adsorption affinity towards oxygen.<sup>144</sup> The effect of surface area was further optimized by developing high surface area ZrO<sub>2</sub> and Ru/ZrO<sub>2</sub> catalysts (surface area = 256 m<sup>2</sup> g<sup>-1</sup>) through the evaporation-induced self-assembly (EISA) method but there was no further improvement in the catalyst performance.<sup>145</sup> Ru nanoparticles dispersed over HAP (Ru/HAP) gave the best results with higher stability and recyclability.<sup>146</sup> Although the conversion and yield are selective, the lengthy reaction time (24 h) is the major disadvantage of this process. An increase in catalytic activity and efficiency is

required to reduce the process time by either changing the metal proportion or altering the structure. The catalyst structure strongly demonstrates that the catalytic efficiency and cubic spinel structure are responsible for the effective formation of FDCA from HMF over the Ru/MnCo<sub>2</sub>O<sub>4</sub> catalyst.<sup>144</sup> The reduced yield was observed in the non-cubic spinel structured oxygen deficient Ru/MnCo<sub>2</sub>O<sub>3</sub> catalyst. The importance of such a structure was further confirmed by the oxygen-deficient catalyst (Ru/MnCo<sub>2</sub>O<sub>3</sub>), which obtained only 69.9% FDCA yield under the same process conditions (Table 4).<sup>144</sup> The recycling of Ru/MnCo<sub>2</sub>O<sub>4</sub> was found to be economical without any significant loss. TEM analysis of the spent catalyst showed no discernible change in the structural stability and there was no Ru metal leaching.<sup>144</sup> Moreover, the utilization of the heterogeneous Ru/MnCo<sub>2</sub>O<sub>4</sub> catalyst in the base-free environment is in favor of the green environment protocol. However, the use of CaCO<sub>3</sub> as a cheap base still needs further exploration after the development of FDCA salt recovery methods.<sup>147</sup>

**HMF oxidation to FDCA over Rh-supported catalysts.** Rhodium (Rh) has similar catalytic potential to Au, Pt, and Pd, but this metal has been rarely studied for HMF oxidation to produce FDCA. Only Strasser's group has investigated the role of the Rh/C catalyst for HMF oxidation.<sup>96</sup> The authors compared the performance of different metals supported on C for FDCA formation under high pressure and low temperature. Using the temperature of 50 °C and a higher oxygen pressure of 10 bar resulted in only 12.62% FDCA yield with 82% HMF conversion in 4 hours over Rh/C catalyst. Due to the very low FDCA yield and HMF conversion, there has not been any further research on utilizing Rh-supported metal catalysts in FDCA production.

**HMF oxidation to FDCA over non-noble metal supported catalysts.** Noble-metal catalysts are superior in stability, catalytic activity, recyclability and performance, but the large-scale utilization of these catalysts seems to be imprudent due to their high cost and poor availability. Research on inexpensive non-noble metal catalysts has progressed through the development of stable and active transition metal catalysts for industrial applications.<sup>88</sup> The stable iron(III)-porous organic polymer, (Fe-POP), was developed and applied in the aerobic oxidation of HMF.<sup>149</sup> High HMF conversion and FDCA yield further inspired the development of non-noble metal catalysts. Merrifield resin-supported Co(II)-meso-tetra(4-pyridyl)-porphyrin (abbreviated as Merrifield Resin-Co-Py) catalyst was

**Table 5** Oxidative production of FDCA from HMF over non-noble metal heterogeneous catalysts

Catalyst	Oxidizing agent	Oxidation environment	Temp. (°C)	Time (h)	HMF. Conv. (%)	FDCA yield (%)	Ref.
Fe-POP	10 Bar O <sub>2</sub>		100	10	100	79	149
Merrifield resin-Co-Py	<i>t</i> -BuOOH	Acetonitrile	100	24	95.6	90.4	150
Li <sub>2</sub> CoMn <sub>3</sub> O <sub>8</sub> /NaBr	55 Bar air	Acetic acid	150	8	100	80	151
nano-Fe <sub>3</sub> O <sub>4</sub> -CoOx	—	—	80	12	97.2	68.6	152
Fe <sub>0.6</sub> Zr <sub>0.4</sub> O <sub>2</sub>	20 Bar O <sub>2</sub>	[Bmim]Cl	160	24	99.7	60.6	67
Ce <sub>0.5</sub> Fe <sub>0.5</sub> O <sub>2</sub>	20 Bar O <sub>2</sub>	[Bmim]Cl	140	24	98.4	13.8	154
Ce <sub>0.5</sub> Zr <sub>0.5</sub> O <sub>2</sub>	20 Bar O <sub>2</sub>	[Bmim]Cl	140	24	96.1	23.2	154
Ce <sub>0.5</sub> Fe <sub>0.15</sub> Zr <sub>0.35</sub> O <sub>2</sub>	20 Bar O <sub>2</sub>	[Bmim]Cl	140	24	99.9	44.2	154
MnCo <sub>2</sub> O <sub>4</sub>	20 Bar O <sub>2</sub>	8.34 m KHCO <sub>3</sub>	100	24	99.5	70.9	155

developed and applied, and it demonstrated a higher FDCA yield (90.4%) with complete HMF conversion (Table 5).<sup>150</sup> Kinetically, HMF oxidation proceeds through the DFF route (Scheme 3, route B) and the recycling experiments produced pleasing results. Spinel mixed metal oxide catalyst (Li<sub>2</sub>CoMn<sub>3</sub>O<sub>8</sub>), with sodium bromide (NaBr) and acetic acid as additives, gave adequate yield but high temperature, pressure and additive (NaBr and acetic acid) requirements have made this process less competitive for industrial application.<sup>151</sup> Large-scale production processes always prefer low temperature and pressure due to safety, energy and economic concerns.

The recovery and recycling ability of the catalyst were further addressed by producing the magnetic nano-Fe<sub>3</sub>O<sub>4</sub>-CoO<sub>x</sub> catalyst.<sup>152</sup> In spite of the higher HMF conversion (97.2%), the obtained yield of FDCA is only 68.6% (Table 5). Although the yield is low, this method initiates the utilization of transition metal catalysts instead of the highly expensive noble metal catalysts with the added advantages of magnetic separation. Experiments have proved that HMF oxidation to FFCA, the first step of oxidation, is initiated by the Brønsted base even in the absence of a catalyst, while FFCA oxidation to FDCA only takes place over the catalyst. The inexpensive heterogeneous catalyst (Mn<sub>0.75</sub>/Fe<sub>0.25</sub>) works efficiently at high pressure (8 bar air) and the observed yield can be as high as 99% of FFCA at moderate temperature (90 °C).<sup>153</sup> Hence, it was elucidated that the two-step oxidation, HMF to FFCA and FFCA to FDCA, may generate better conversion and selectivity with no catalyst deactivation.

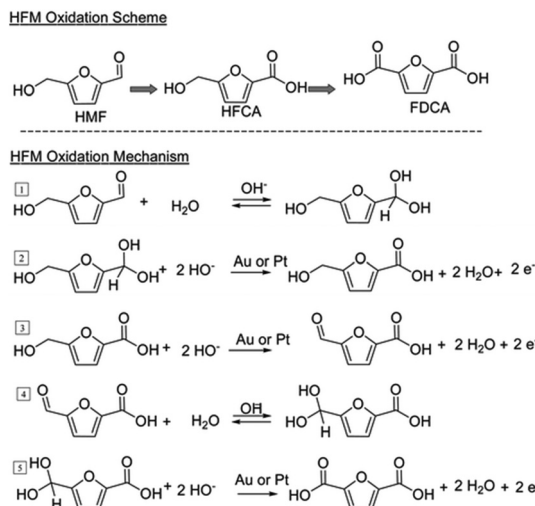
Ionic liquids (ILs) have also been investigated as a reaction medium along with inexpensive mixed oxide catalysts.<sup>154</sup> Pure metal oxides (Fe<sub>2</sub>O<sub>3</sub>, ZrO<sub>2</sub>) and their numerous combinations (Fe/Zr ratio) are in use for catalyst development. The FDCA yield is low irrespective of higher HMF conversion with all proportions and changing process parameters seems not to improve the catalyst performance (Table 5).<sup>154</sup> Other catalysts were developed with different combinations of Mn and Co oxides.<sup>155</sup> Highly selective results have been obtained by applying the nanoscale center-hollowed hexagon MnCo<sub>2</sub>O<sub>4</sub> spinel to catalyze the oxidation of HMF because of its efficient reducibility and oxygen mobility (Table 5).

The ILs and non-noble metal catalyst combination is less attractive due to low FDCA yield and environmental concerns at this stage. However, increases in performance with changed

combinations reveal the scope for further process and catalyst development.<sup>156,157</sup> Researchers are continuously investigating the development of novel inexpensive transition metal catalysts and green solvents for quantitative yields of FDCA with green properties.<sup>158,159</sup>

**Mechanism of HMF oxidation over metal catalysts.** All the discussed mechanisms for HMF oxidation are based on the stepwise oxidation of aldehyde and alcohol functional groups. The reactions proceed by either the preferred oxidation of alcoholic functional groups (Scheme 3, route A) or aldehyde groups (Scheme 3, route B). Many researchers have discussed the reaction mechanisms for the catalyst used and have primarily agreed on the formation of FFCA in the second step and DFF and HFCA as competitive process intermediates in the first step (Scheme 3).

Davis *et al.* applied the isotope labeling technique to evaluate the exact HMF oxidation mechanism over noble metal catalysts.<sup>160,161</sup> The Au/TiO<sub>2</sub> catalyzed oxidation of HMF in alkaline medium can produce HFCA with higher selectivity ( $\geq 98\%$ ) under 3.45 bar oxygen pressure at 22 °C. The oxygen isotope <sup>18</sup>O<sub>2</sub> has been used as an oxidant to investigate the role of oxygen. Alkaline medium reaction products were analyzed for the oxygen isotope and the results surprisingly elucidated that there was no <sup>18</sup>O<sub>2</sub> isotope in the HFCA molecule. This discrepancy indicates that oxygen is incorporated from solvent water rather than the available oxidant (oxygen). These findings were then further confirmed by employing labeled water (H<sub>2</sub><sup>18</sup>O) as a solvent.<sup>161</sup> On analysis, two isotopes of oxygen (<sup>18</sup>O) were found to be integrated into Na-HFCA and HFCA structures, hence, O<sub>2</sub> is not essential as an oxidant for the oxidation of the aldehyde functional group. Aldehyde side groups present in the HMF molecule are rapidly oxidized to the geminal diol through reversible nucleophilic addition. The nucleophilic addition of OH<sup>-</sup> to carbonyl radicals and the simultaneous proton transfer from water molecules produces unstable intermediates (Scheme 10, step 1);<sup>161</sup> hence, two oxygen atoms from water molecules are incorporated into the HMF processing intermediates, which can be confirmed by the presence of <sup>18</sup>O when H<sub>2</sub><sup>18</sup>O is applied as a solvent. Geminal diol dehydrogenation promoted by the adsorbed OH<sup>-</sup> on the catalyst surface results in the formation of COOH in the second step (Scheme 10, step 2), and the aldehyde functional group of HMF is successfully oxidized to carboxylic acid. This proves that the reaction mechanism follows route A of Scheme 3,



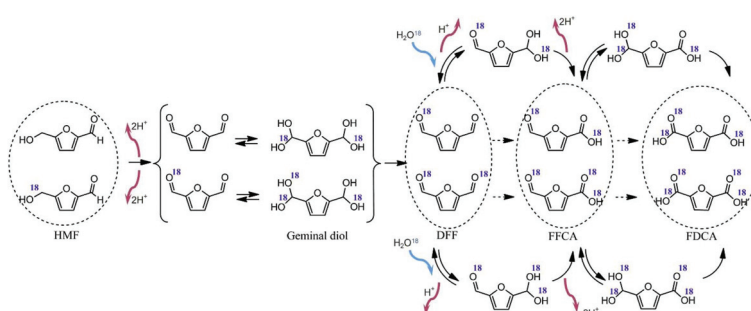
**Scheme 10** Reaction mechanism of the aqueous phase oxidation of HMF in alkaline medium over metal (Pt/Au) catalyst.<sup>160,161</sup>

being similar to that found in previous studies.<sup>162,163</sup> Furthermore, the oxidation of alcoholic groups present in HFCA is required to obtain FDCA. The presence of a base is vital for the oxidation of the alcoholic group, regardless of what catalyst is applied. The base-initiated deprotonation of alcoholic groups produces alkoxy intermediates.<sup>164</sup> Base-donated hydroxide ions adsorbed on the catalyst surface then activate the O–H bonds of alcoholic side chains to produce the aldehyde intermediate (FFCA) (Scheme 10, step 3). The next steps are the oxidation of the aldehyde groups (Scheme 10, steps 4 and 5), which proceeds quite similarly to those in the previous discussion. Again, two oxygen atoms are fused when water, having the oxygen isotope ( $\text{H}_2^{18}\text{O}$ ), is used for the synthesis of the geminal diol from the reversible hydration of the aldehyde group. The complete oxidation of HMF to produce FDCA can be well explained, indicating that oxygen is incorporated from water molecules instead of the freely available molecular oxygen (the oxidant). However, the presence of molecular oxygen or any other oxidizing agent is necessary for the oxidative production of FDCA from HMF to indirectly facilitate the oxidation process by removing electrons deposited on the catalyst surface.<sup>160,161</sup>

Scheme 10 elucidates that the reaction mechanism of HMF oxidation is facilitated by the presence of the base-provided hydroxyl ion ( $\text{OH}^-$ ). However, this suggested mechanism works only in the presence of a base, while base-free HMF oxidation proceeds with a different mechanism. The base-free oxidation mechanism was investigated by Yan's group over a poly [bvbim]Cl-stabilized Pd (PVP) catalyst using similar isotope labeling technology (Scheme 11).<sup>103</sup> Isotope labeling confirmed the presence of DFF and FFCA as process intermediates rather than HFCA in base-free oxidation.<sup>103</sup> The same mechanism has also been confirmed by others using low pH or base-free environments.<sup>132,161</sup> Similarly, the isotope labeling technique ( $\text{H}_2^{18}\text{O}$ ) has been utilized to interpret the reaction mechanisms of HMF oxidation over Pt/PVP catalyst. FFCA and FDCA were recorded as oxidation end products and the presence of  $^{18}\text{O}$  atoms was confirmed by mass spectra.<sup>103</sup> The peaks with  $m/z$  161 and 163 relate to the  $^{18}\text{O}$ -labelled FDCA, while peaks with  $m/z$  143 and 145 relate to the  $^{18}\text{O}$  labeled FFCA. Being analogous to the base-promoted oxidation step 1 (Scheme 10, step 1), nucleophilic addition of  $\text{H}_2\text{O}$  to carbonyl rapidly produces the geminal diol *via* the reversible hydration of the aldehyde groups (Scheme 11).<sup>103</sup> In the end, the carboxylic groups are regenerated by the migration of two protons to the metal surface and water by reactions between molecular oxygen and surface hydrides; therefore, the base-free oxidation of HMF takes place completely.<sup>103</sup>

Even though the reaction mechanism for the oxidative production of FDCA from HMF can be well interpreted by the isotope labeling technique, extensive work is still required to study the chemical kinetics and reaction mechanism in depth. The utilization of modern techniques for determining the comprehensive intrinsic kinetic mechanism will help with the understanding of the synthesis process. This solid insight into the reaction pathway will help researchers with the development of new, efficient and stable green catalysts and solvent systems, which are necessary for the rational design of the catalysts and the production process.

**HMF oxidation to FDCA over metal-free nano-porous graphitic carbon catalysts.** Initially, metal-free catalysts were considered inactive for HMF oxidation and were not applied till the development of the non-metallic zeolitic-imidazole structure (ZIF-8), which is imitative of nitrogen-incapacitated nano-



**Scheme 11** Integration of  $^{18}\text{O}$  into the reaction steps.  $^{18}\text{O}$  is shown in blue and the observed units are in dashed ellipses.<sup>103</sup>

porous carbon (denoted as NNC).<sup>165</sup> Catalysts were named NNC-X (X-represents the carbonization temperature) after carbonization and calcination under an inert atmosphere. The catalyst properties such as the graphite-carbon framework, specific surface area, and porosity are controlled by calcination and the carbonization mechanism.<sup>165</sup> NNC-900 gave the highest yield of FDCA (80%) with complete conversion of HMF at 80 °C using pure oxygen under atmospheric pressure in alkaline medium. The oxidation reaction proceeds *via* the HFCA and FFCA route (Scheme 3, route A) over NNC-900 catalyst with the first step being a fast step.<sup>165</sup> Increasing temperature accelerates the HMF conversion, signifying the temperature dependency of the fast step, whereas, the conversion of HFCA and FFCA to FDCA are recognized as the rate determining steps (slow steps). These findings are in good agreement with previously published results indicating the same route and kinetics.<sup>94,165</sup>

One of the most important selective aspects of heterogeneous catalysts is that the catalyst can be easily separated and recycled for multiple runs. The quaternary nitrogen (N-Q) configured NNC-900 catalyst was separated using centrifugation, washed with deionized water and methanol, dried at 150 °C for 5 hours prior to each run. The recorded decrease in FDCA yield was 12.5% in the fourth run (1<sup>st</sup> 80% and 4<sup>th</sup> about 70%).<sup>165</sup> There was no significant structural change except for a minor change in the N-Q amount. This result indicates the selective separation and recycling efficiency of the catalyst applied. A long reaction time and low HMF/base ratio make it less competitive for industrial applications but, further research can improve the potential of this green and economical heterogeneous catalyst system for HMF oxidation.

### One-pot production of FDCA from biomass

Direct conversion of biomass and biomass fractions into the required products is always a fascinating and economical alternative for industrial application.<sup>166,167</sup> The conversion of HMF to FDCA is technically feasible but faces problems of cost, stability and availability.<sup>168</sup> There are also many other potential and more economical uses of HMF that barricade its oxidation to produce FDCA.<sup>169,170</sup> HMF is a biomass-derived product so the direct synthesis of FDCA from carbohydrates such as fructose, glucose, cellulose and lignocellulosic biomass has been researched for a long time.<sup>171</sup> This conversion process is termed a one-pot synthesis (Fig. 2) and is generally carried out with combined acidic and metal site multifunctional catalysts. The competitive oxidation of carbohydrates is a major hurdle for the direct production of FDCA from carbohydrates but it can be partially resolved by applying molecular sieves or polymeric membranes in biphasic systems.<sup>172,173</sup> The preferred oxidation of carbohydrate is vetoed by using polytetrafluoroethylene membrane (pore size = 0.45 µm and exchange area = 70 cm<sup>2</sup>) as a reactor divider in the water and MIBK system (Fig. 3).<sup>172</sup> HMF is produced on a solid acid catalyst (Lewatit SPC 108) by the dehydration of fructose passed through the membrane toward the MIBK solution and oxidized to FDCA over metal base catalysts. Single phase

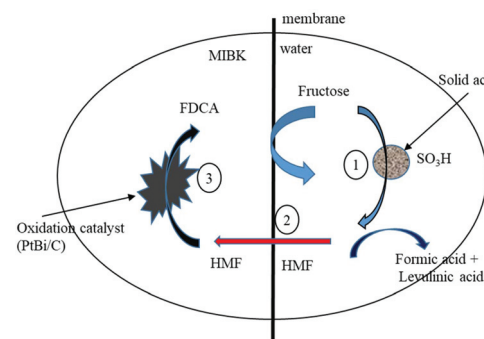


**Fig. 3** Membrane reactor processing scheme: (1) water phase HMF synthesis; (2) HMF diffusion in the MIBK phase; (3) HMF oxidation to FDCA. (Adapted from ref. 172).

conversion in MIBK only produces DFF so the presence of water is necessary for the conversion of the alkoxy group to FDCA.<sup>172</sup> A higher yield (25%) of levulinic acid and its diffusion through the membrane leads to lower FDCA yield.<sup>172</sup> Although this one-pot yield is very low and challenging, together with purification difficulties, it unwraps a new research arena.

A bifunctional catalyst (encapsulation of Co(acac)<sub>3</sub> in sol-gel silica) increased the fructose conversion and product selectivity, which was further improved by a one-pot two-step process.<sup>174,175</sup> Fructose was dehydrated to HMF in the HCl-catalyzed isopropanol mixture and was then oxidized to FDCA in the second step.<sup>175</sup> This particular process has the benefits of high overall yield (83%) and efficient solvent (isopropanol) recovery. The water extraction of FDCA from the product mixture quantitatively affects the product yield, and water extraction followed by oxidation over Au/HT catalyst is the most economical purification methodology with the maximum yield (98%).<sup>175</sup> In contrast, the replacement of the catalyst with solid polybenzyl ammonium chloride decreases the overall yield.<sup>176</sup> The biphasic system was then modified to the triphasic system by introducing tetraethylammonium bromide (TEAB) as phase I, MIBK as phase II and water as phase III.<sup>177</sup> In this triphasic system, phase I eases the dehydration of sugars (fructose or glucose) to HMF which is then extracted, refined, and transported to phase III through a channel (phase II). The Au/HT catalyst used in phase III improved the HMF oxidation. When fructose was used as feedstock, the FDCA yield was high (78%) but was reduced to 50% with glucose.<sup>177</sup> The one-pot one-step process can be developed into a one-pot two-step process to improve the yield and selectivity.<sup>178</sup> This process facilitates the catalyst recovery and recycling for economic expansion to mass production. The nanocatalyst ( $\text{Fe}_3\text{O}_4\text{-CoO}_x$ ) efficiently oxidizes HMF to FDCA utilizing *t*-BuOOH as an oxidant.<sup>178</sup> HMF was produced from fructose over an acid catalyst ( $\text{Fe}_3\text{O}_4@\text{SiO}_2\text{-SO}_3\text{H}$  in DMSO) followed by the oxidation to FDCA with *t*-BuOOH over the nano- $\text{Fe}_3\text{O}_4\text{-CoO}_x$  catalyst.<sup>178</sup> An external magnet can separate the catalyst before HMF oxidation. Although the observed FDCA

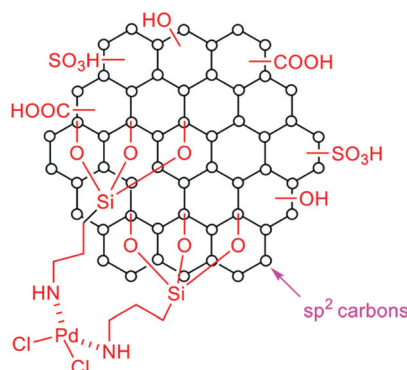


Fig. 4 Schematic representation of the Pd/CC catalyst (adapted from ref. 116).

yield is low (59.8%), the ease of separation and efficient recycling are the added advantages.<sup>178</sup> Glucose dehydration with FDCA over iPrOH/H<sub>2</sub>O or THF/H<sub>2</sub>O produces quantitative yield in comparatively less time.<sup>179</sup> The green Pd/CC catalyst (Fig. 4) developed by the carbonization of biomass-derived glucose works efficiently in the one-pot two-step synthesis of FDCA from glucose. A more efficient, green, and commercial process has been reported to produce FDCA with a yield of 64% without any separation and purification requirements.<sup>116</sup> The developed catalyst showed profound separation and recycling efficiency with extended stability. The Pt/C catalyst worked efficiently (91% FDCA yield) with high initial fructose concentrations (15 W%) in a co-solvent system of  $\gamma$ -valerolactone (GVL) in water (GVL/H<sub>2</sub>O).<sup>107</sup> Fructose can be dehydrated to HMF in 50% aqueous solution of GVL using the separated FDCA product solution as the acid catalyst, followed by oxidation over Pt/C catalyst. This process has industrial potential as the produced FDCA is easy to separate by crystallization. The clean solution can be recycled to the fructose dehydration step for economical reasons.<sup>107</sup> This efficient recycling of the spent liquor reduces the need for external acid catalyst together with the elimination of the separation step and minimizes waste, thus conforming to the green chemistry.

So far, the one-pot production of FDCA is mostly focused on the utilization of fructose as feedstock. The FDCA yield by the one-pot process with glucose as the feedstock is usually lower than with fructose because the isomerization of glucose to fructose is involved in the process. Much lower yield is achieved for one-pot processing of the lignocellulosic biomass primarily due to the difficulty of releasing glucose from the cell wall matrix. Although the one-pot process is a new trend in the research arena, it has the obstacles of low FDCA yield with less competitive and economic constraints.<sup>88</sup> Further development of the one-pot process is needed in terms of yield, selectivity and economics. Therefore, the development of new transition metal catalysts is necessary for the economical utilization of this concept. Side reaction elimination and FDCA yield enhancement can be accelerated by the isolation of multiple catalytic sites. Thus, the developed catalyst must have

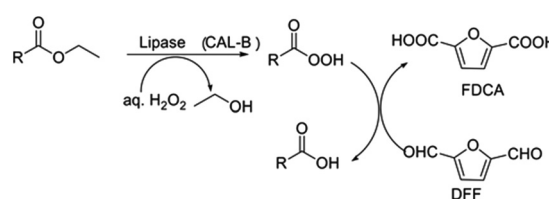
hydrophilic acidic sites for the preferred adsorption of carbohydrate. This will promote the dehydration of carbohydrate to HMF and then release this product to the reaction mixture. Active oxidative sites present in a hydrophobic environment can improve the adsorption of the available HMF that will intensify its conversion to FDCA. This simultaneous process will enhance the process yield and selectivity to make the one-pot process more feasible, selective, reliable and cost competitive.

#### Biocatalytic production of FDCA from HMF

Biochemical transformation is more advantageous in terms of process parameters than chemical conversions as these processes are usually performed under mild conditions. There is also the tendency for relatively non-toxic intermediates and by-product formation in biocatalytic processes. Therefore, the use of biologically active catalysts and biological cell sequencing technology is needed for the production of biochemicals in current environment sensitive scenarios.<sup>180</sup> Similarly, the production of FDCA from HMF and other biochemical intermediates on bioactive catalysts is always interesting but challenging for the research community.<sup>181</sup> In spite of all these associated incentives, the biocatalytic routes for FDCA production has not yet been well established.

The biocatalytic conversion of DFF to FDCA is usually conducted by pouring an aqueous solution of hydrogen peroxide (30%) into the mixture of alkyl esters (alkyl donor) and lipases (biocatalyst), which produces peracid and subsequently oxidizes DFF to FDCA.<sup>182</sup> High FDCA yield (>99%) and selectivity (~100%) has been observed in the DFF oxidation process (Scheme 12) but this biocatalytic system is inactive for HMF oxidation. The use of DFF for the production of FDCA is uneconomical as HMF conversion to DFF is an additional step in this model.<sup>182</sup> A chloroperoxidase from *Caldariomyces fumago* has been found to have the potential of HMF bio-oxidation but this process is also uneconomical due to the low FDCA yield (60–75%) and the higher competitive yield of HFCA (25–40%).<sup>183</sup> FDCA produced with HFCA cannot be purified to such a degree for polymerization so *C. fumago*-derived chloroperoxidase is not yet good enough for the biosynthesis of FDCA from HMF.<sup>183</sup>

A fermentative synthesis process of HMF to FDCA with *Pseudomonas putida* S12 biocatalyst to facilitate the oxidoreductase from *Cupriavidus basilensis* HMF14 has been investigated using glycerol as a carbon source.<sup>184</sup> FDCA yield of 97% (from

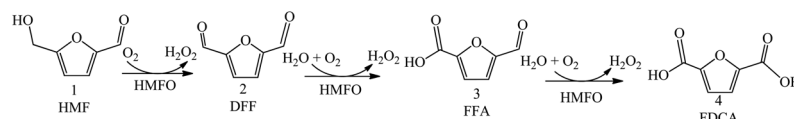


Scheme 12 DFF oxidation to FDCA through *in situ* lipase-catalyzed peracid formation.<sup>88,182</sup>

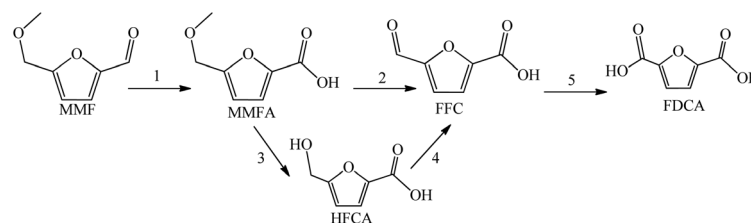
HMF feedstock) with 99.4% solid recovery was obtained from the culture broth. This model proceeds *via* the activities of both dehydrogenases and oxidases.<sup>184</sup> Usually, enzymes are either aldehyde oxidant or alcohol oxidant, whereas complete oxidation of HMF requires an enzyme reactive enough to oxidize both the aldehyde and alcohol groups. Hexamethyl furfural oxidase (HMFO) from glucose-methanol-choline oxidoreductase (GMC) has been identified as having superior oxidation potential at ambient conditions, satisfying this requirement.<sup>185</sup> Although the yield is very high (95%), the low feedstock concentration (2 mM) and long reaction time (24 hours) make this strain less attractive.<sup>88</sup> Catalytically active and stable strains, *Methylobacterium radiotolerans* (G-2) and *Burkholderia cepacia* (H-2) have been applied in the biotransformation of HMF to FDCA.<sup>186</sup> Under the optimal conditions with 3% cell biomass, the isolated strain *B. cepacia* could produce FDCA of 1276 mg L<sup>-1</sup> from 2000 mg L<sup>-1</sup> of HMF.<sup>186</sup> An increase in temperature accelerates the biotransformation rate, while the optimal temperature (28 °C) is used for the biotransformation of HMF to FDCA.<sup>186</sup> Increasing the concentration of HMF can increase the FDCA yield but the recovery is inefficient at higher concentration. A lower concentration (<1500 mg L<sup>-1</sup>) can support minimal cell growth, while higher concentrations (>2000 mg L<sup>-1</sup>) reduce the cell density due to the increased HMF toxicity at higher concentration. The produced FDCA also results in reduced pH, which is also unfavorable for cell growth. Hence, 2000 mg L<sup>-1</sup> is the optimum HMF concentration for maximum FDCA yield when using *B. cepacia*. More concentrated FDCA (11.3 g L<sup>-1</sup>) can be obtained by the strain *R. ornithinolytica* BF60 (@45 g L<sup>-1</sup>) with HMF conversion of 89% at 30 °C in a slightly basic medium (pH = 8, with 50 mM phosphate buffer).<sup>187</sup> These biocatalysts are very sensitive to the feed concentration and pH of the medium, so precise process control is mandatory for efficient production.

With the approach of a robust biocatalyst, genetically modified strains incorporating HMFO and HmfH with *R. ornithinolytica* BF60 have been developed to achieve the

benefits of the simultaneous oxidation of the aldehyde and alcoholic group.<sup>188</sup> ROBF60-H (expressing HmfH), ROBF60-O (expressing HMFO) and ROBF60-HO (expressing both HmfH and HMFO) have been applied successfully in analogous environments and strain ROBF60-HO could provide maximum HMF conversion (93.6%).<sup>188</sup> HMF toxicity could be reduced by increasing the biomass concentration to keep the catalyst biologically active and alive.<sup>189</sup> During biotransformation, strain ROBF60-H initially converted HMF into HMF-alcohol in 24 hours then oxidized it to FDCA. The cultured strain (ROBF60-H) behaved similarly to the wild strain, and HMF-alcohol and HMF concentrations diminished quickly after 24 hours.<sup>188</sup> Strain ROBF60-O also followed the same route with a faster rate and converted HMF to the HMF-alcohol complex in 12 hours. Similarly, strain ROBF60-HO also used a pattern analogous to ROBF60-H with little accumulation of HMF and HMF-acid.<sup>188</sup> The maximum yield of FDCA was obtained by *R. ornithinolytica* BF60.<sup>188</sup> Although this biocatalytic process is simple and eco-friendly, the low yield makes it less attractive for larger scale production. Catalytic performance and stability of the newly developed HMFO from *Methylovorus* sp. were further exploited by using the recently-developed FRESCO method (a computational approach to identifying thermostabilizing mutations in a protein structure).<sup>188</sup> HMFO developed with FRESCO in combination with the gene shuffling approach can tolerate the presence of co-solvents and additional mutants. Due to its stability and catalytic efficiency, the final HMFO variant appears to be a promising catalyst for the industrial-scale production of FDCA from HMF. Quantitative FDCA yield can be obtained using the 8BxHMFO variant (Scheme 13).<sup>190</sup> Another substrate, methoxymethylfurfural (MMF) can be oxidized to FDCA using the enzyme cascade of aryl-alcohol oxidase (AAO), unspecific peroxxygenase (UPO) and methanol oxidase (MOX).<sup>191</sup> AAO converts MMF to MMFA, slowly releasing 1 equivalent of H<sub>2</sub>O<sub>2</sub> (Scheme 14, step 1), and UPO selectively cleaves the ether linkage of MMFA to produce FFC (Scheme 14, step 2), con-



Scheme 13 Oxidation reaction of 5-hydroxymethylfurfural (HMF) to 2,5-furandicarboxylic acid (FDCA) by HMFO.<sup>190</sup>



Scheme 14 Oxidation pathways of MMF into FDCA with cascade enzymatic catalysts.<sup>191</sup>

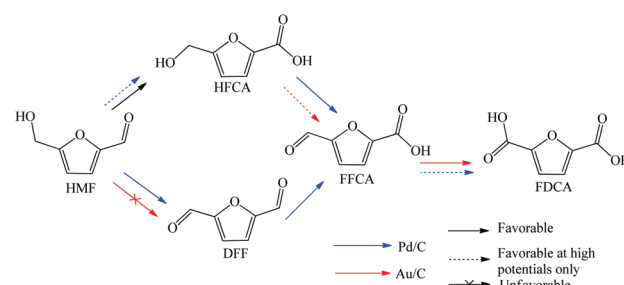
suming the  $\text{H}_2\text{O}_2$  present in the system. HFCA was observed in very low proportions, indicating that the FFC route (step 2–5) is the main reaction pathway.<sup>191</sup> MOX catalyzes the canonical reaction and produces  $\text{H}_2\text{O}_2$  from  $\text{O}_2$  by the concomitant catalytic oxidation of methanol to methanal, thus increasing the FDCA yield to 70%.<sup>191</sup> HmfH and HMFO potentially catalyze the oxidation of aldehyde and alcoholic groups, respectively, and can work well for a wide substrate spectrum.<sup>191,192</sup>

Although the biocatalytic yield of FDCA is low and the process is uneconomical at this stage, this process still conforms to green environment protocols. Further research in this field with the development of robust biocatalysts can make this route more attractive. Biocatalysis is usually depressed by harsh process environments so ambient temperature and atmospheric pressure are generally enough to proceed. Currently, the biotransformation of HMF to FDCA is performed with lower feedstock concentration for long processing time and the need for sophisticated control. Genetic engineering and gene sequencing for the production of biocatalysts with enhanced catalytic activity, stability at fluctuating process conditions and the ability to digest high HMF concentration will increase the industrial potential of this process. The ‘construction’ of microorganisms with multiple enzymatic functionalities, especially the direct conversion of carbohydrates to FDCA, is now an exciting but challenging topic for researchers. It will not only make the FDCA cost competitive but will also increase the production level for sustainable market supply.

### Electrolytic production of FDCA from HMF

Electrochemical transformation is always considered important as a clean and green technology because the process is driven only by the electrochemical potential. Electrochemical oxidation of HMF to produce FDCA under mild conditions proceeds through electron migration thus eliminating the need for any external oxidant. This conversion methodology is now gaining scientific interest due to environment and energy sensitivity.<sup>193</sup> Control of the faradaic efficiency and oxidation potential are added advantages of this process, which can facilitate monitoring of the thermodynamic properties, surface chemistry of the reaction and ultimately the rate of reaction.<sup>194</sup>

Primarily, H-shaped electrochemical cells were used for the first time (1995) for HMF oxidation to FDCA (Fig. 3) using nickel oxide/hydroxide as the anode and NaOH solution as the alkaline media.<sup>193</sup> The electrochemical oxidation of HMF could take place at the anode, yielding 71% of FDCA in 4 hours at a current density of  $0.016 \text{ A cm}^{-2}$ . However, further extensive research on the electrochemical oxidation of HMF has not been conducted. Perhaps the importance of FDCA as a green building block has not been explored and the potential of this process has not been thoroughly considered. Now, after the aggressive enforcement of green environment protocols and the utilization of green polymer production processes, researchers are expansively searching for eco-friendly and economical models for FDCA synthesis. This shift elaborates the importance of the electrochemical process as a green technology, especially for polymer production. Regardless of



**Scheme 15** Proposed reaction route for the oxidative production of FDCA from HMF using Au/C and Pd/C electrocatalysts in alkaline medium.<sup>80</sup>

all its benefits, this process has not yet been thoroughly investigated. The Pt electrode was once used with current density of  $+0.44 \text{ mA cm}^{-2}$  but the recorded FDCA yield was very low (18%) with only 70% HMF conversion, and the competitive electrolysis of  $\text{H}_2\text{O}$  to parent oxygen and hydrogen was recognized as a limiting reaction.<sup>96</sup> Li *et al.* subsequently reported the electrochemical production of FDCA using carbon black-supported noble metal catalyst in alkaline medium.<sup>80</sup> Aldehyde oxidation was faster than alcohol oxidation over Au/C catalyst. Higher electrochemical potential is required for preferred alcohol oxidation; hence, the intermediate FFCA produced with DFF or HFCA depends on the electrode and electrode potential (Scheme 15).<sup>80</sup> Au/C produces HFCA under lower electrode potential and further oxidation to FDCA requires higher potential, whereas Pd/C-catalyzed reactions follow two different routes with changed electrode potential.<sup>80</sup> At low electrode potential, the oxidation rate of the aldehyde group is lower on Pd/C than Au/C but significantly enhanced with increased potential. Bimetallic (Pd–Au) produces higher FFCA and FDCA than monometallic catalysts at lower electrode potential. Further, the PdAu<sub>2</sub>/C bimetallic catalyst yields 83% FDCA with 100% HMF conversion at the electrode potential of 0.9 V, showing the effect of alloying metals on the enhancement of the FDCA yield. However, this process produces FDCA in a mixture with other oxidative products and purification is very difficult and uneconomical.

The use of 2,2,6,6-tetramethylpiperidine-1-oxyl (TEMPO) as a mediator greatly reduces the over potential requirements for HMF oxidation by suppressing water oxidation.<sup>96,193</sup> The electrochemical cell used by Choi is shown in Fig. 5a and the reaction pathway over TEMPO is shown in Scheme 16.<sup>193</sup> The Au electrode oxidized TEMPO to TEMPO<sup>+</sup>, which served as an oxidizing catalyst and achieved high FDCA yield ( $\geq 99\%$ ) with  $\geq 93\%$  faradaic efficiency in alkaline solution (pH 9.2). In the electrochemical oxidation of HMF, a photoelectrochemical cell (PEC) with nanoporous n-type BiVO<sub>4</sub> electrode (photo-anode) and Pt-electrode (cathode) was fabricated (Fig. 5b).<sup>193</sup> The photoanode generates and separates electron–hole pairs by absorbing photons, then the electron–hole pairs are transmitted to the Pt-cathode. At the Pt-cathode, water is reduced to hydrogen gas (eqn (I)), whereas holes, after reaching the BiVO<sub>4</sub> surface, proceed with the HMF oxidation through TEMPO

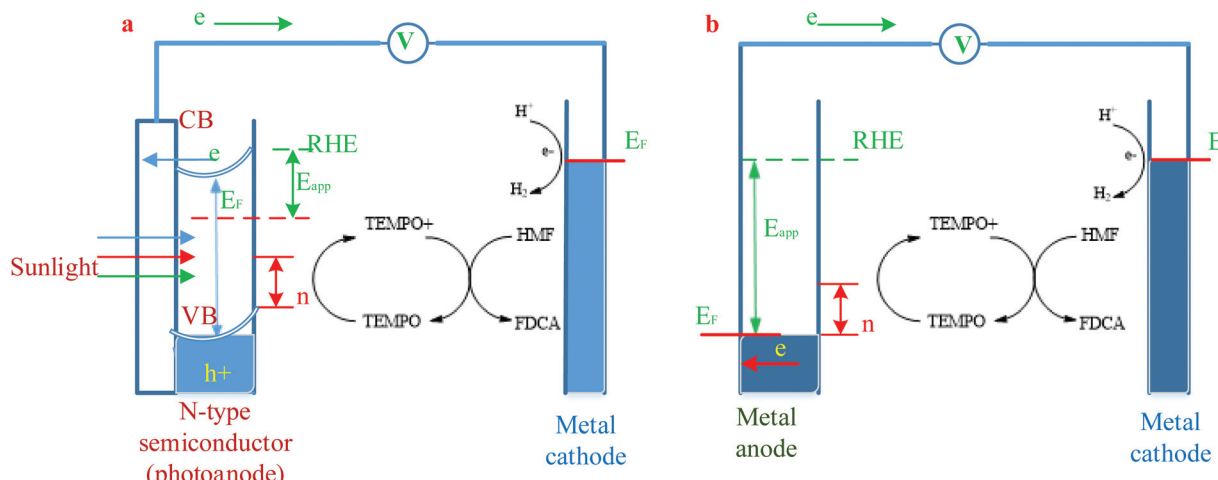
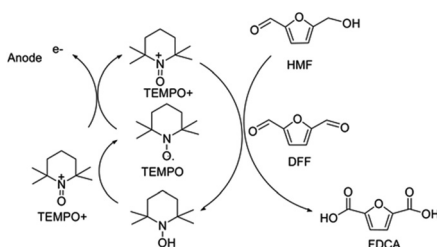


**Fig. 5** Electrochemical and photoelectrochemical cell comparison: (a) photoelectrochemical TEMPO facilitated FDCA production from HMF; (b) electrochemical TEMPO facilitated FDCA production from HMF. EF, Fermi energy; CB, conduction band (adapted from ref. 193).



**Scheme 16** The TEMPO pathway facilitated the electrolytic synthesis of FDCA from HMF.<sup>193</sup>

(eqn (II)). Eqn (III) illustrates the overall cell reaction for FDCA production.<sup>193</sup> This production process has the advantages of higher yield and better faradaic efficiency without any in-process pH adjustment. Additionally, H<sub>2</sub> gas produced separately by water splitting on the cathode can serve as a clean and green source of energy. A greater proportion of TEMPO (1.5 equivalent) is required for higher FDCA yield, making the process highly expensive.<sup>193</sup> Moreover, the separation and purification of FDCA from TEMPO, electrolyte and process byproducts are difficult.<sup>88</sup> Additionally, high FDCA yield can be obtained only by using a low initial concentration of HMF, so the design of more robust electro-catalysts with efficient HMF conversion and high FDCA selectivity is critical. The newly developed Co-P as electrocatalyst and the Co-P/CF electrode can achieve a 99% yield of FDCA with 100% faradaic efficiency.<sup>193</sup> Similarly, the Ni-Fe layered double hydroxide (LDH) nanosheets grown on carbon fiber paper produced a quantitative yield (98%) with 99.4% faradaic efficiency.<sup>195</sup> These processes have the advantages of separating FDCA production at the anode and clean H<sub>2</sub> at the cathode, similar to Choi's finding.<sup>193,196</sup> This process was then modified and patented by Wisconsin alumni research foundation (WARF) Madison, US.<sup>197</sup> Ni-Fe-LDH promotes HMF oxidation under lower potential (1.23 V) compared to water electrolysis and is, therefore, more efficient and sustainable.<sup>195</sup>

Cathode reaction:



Anode reaction:



Inclusive reaction:



During the electrochemical production of FDCA, the process intermediate, FFCA, produced either by the DFF or HFCA route, can be oxidized to FDCA. However, all these process intermediates (DFF, HFCA and FFCA) remain at very low concentrations throughout the process (Table 6).<sup>196</sup> Negligible amounts of HFCA present in the final product solution indicate that the production proceeds through the DFF intermediate (Scheme 3, route B) and the final product FDCA is obtained as a white precipitate at pH 0 (addition of H<sub>2</sub>SO<sub>4</sub>).

The stability and performance of electrodes can be tested through chronoamperometry. These results have elucidated that Co-P electrodeposited copper foam (Co-P/CF) is an excellent and stable electrocatalyst for the production of FDCA in an alkaline medium. This system simultaneously produces H<sub>2</sub> by water splitting at low voltage (1.44 V and current density 20 mA cm<sup>-2</sup>), whereas independent water splitting and H<sub>2</sub> production require 1.54 V.<sup>196</sup> The simultaneous production of FDCA and H<sub>2</sub> is quite inspiring in the current green energy and environment sensitive scenario.<sup>197</sup> A novel continuous electrochemical process of HMF oxidation and integrated product (FDCA) separation using non-noble metal Ni/NiOOH foam electrodes seems to have solved the problem of yield and continuity.<sup>198</sup> Prospective scale-up can be achieved using the filter press type flow reactor with Na<sub>2</sub>SO<sub>4</sub> buffer (pH = 12) and the Ni/NiOOH foam anode, which can achieve 90% FDCA yield with 80% faradaic efficiency and 95% product separation efficiency.<sup>198</sup> This process has been successfully applied to

**Table 6** Oxidation of HMF and product analysis in the AEM-electrolysis flow cell<sup>80</sup>

Catalyst	Potential [V vs. RHE]	<i>S</i> <sub>DFF</sub> [%]	<i>C</i> <sub>HMF</sub> [%]	<i>S</i> <sub>FDCA</sub> [%]	<i>S</i> <sub>FFCA</sub> [%]	<i>S</i> <sub>HFCA</sub> [%]
Pd/C	0.6	<1	75	11	64	25
Pd <sub>2</sub> Au <sub>1</sub> /C	0.6	<1	87	8	62	30
Pd <sub>1</sub> Au <sub>2</sub> /C	0.6	—	100	25	16	59
Au/C	0.6	—	100	1	<1	98
Pd/C	0.9	—	97	29	<1	70
Pd <sub>2</sub> Au <sub>1</sub> /C	0.9	—	100	64	<1	35
Pd <sub>1</sub> Au <sub>2</sub> /C	0.9	—	100	83	<1	16
Au/C	0.9	—	100	1	<1	98
Pd/C	1.2	—	32	3	26	71
Pd <sub>2</sub> Au <sub>1</sub> /C	1.2	—	82	22	17	61
Pd <sub>1</sub> Au <sub>2</sub> /C	1.2	—	100	36	4	60
Au/C	1.2	—	99	14	5	81

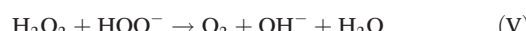
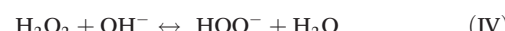
bench-scale production. However, delicate control due to higher pH and construction material are the limitations of this process. Scientists are focusing on elucidating detailed mechanisms and developing robust electrocatalysts to work in a neutral medium ( $\text{pH} = 7$ ).

#### Non-catalytic production of FDCA from HMF

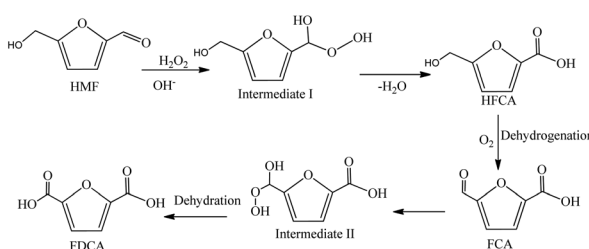
It is always scientifically desirable to shift the conversion processes from catalytic to non-catalytic without disturbing the yield and selectivity, due to financial concerns and availability. Along with the catalyzed production of FDCA, researchers are also continuously struggling to develop a catalyst-free model employing strong oxidizing agents (e.g.  $\text{H}_2\text{O}_2$  etc.).<sup>88</sup> The FDCA yield was optimized in an alkaline medium using different process parameters in a semi-batch reactor. The optimized production of pure FDCA was recorded in 55.6% yield by applying  $\text{H}_2\text{O}_2$  as an oxidizing agent.<sup>199</sup>  $\text{H}_2\text{O}_2$  decomposes to form nascent oxygen ( $\text{O}_2$ ) and  $\text{H}_2\text{O}$  in the alkaline environment through  $\text{HOO}^-$  (eqn (IV) & (V)), which plays a vital role in oxidation.<sup>200</sup>

$\text{HOO}^-$  was produced by the reversible attack of hydroxyl ions ( $\text{OH}^-$ ) on  $\text{H}_2\text{O}_2$  as shown in eqn (IV). Hence, an increase in  $\text{OH}^-$  concentration favors the process in the forward direction and produces more attacking species ( $\text{HOO}^-$ ) for the second step. In alkaline medium, the decomposition of hydrogen peroxide ( $\text{H}_2\text{O}_2$ ) to  $\text{HOO}^-$  in the first step initiates the conversion of the aldehyde group to the carboxylic group present in the HMF structure (Scheme 17, intermediate I). Dehydration of the intermediate I gives HFCA. The *in situ* production of

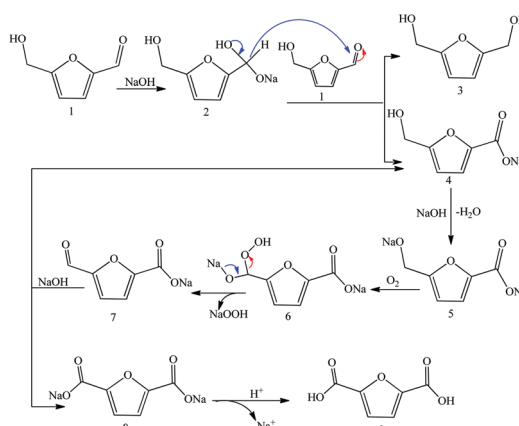
nascent oxygen promotes the FCA formation through the dehydrogenation of HFCA. The aldehyde group present in FCA is further oxidized to intermediate II with a mechanism similar to that of the first step. The dehydration of intermediate II finally yields FDCA. No DFF was detected during the process, which confirms the HFCA route (Scheme 3, route A). Scheme 17 outlines the detailed mechanism.<sup>199</sup>



Considering the advantage of HMF extraction in organic solvent, catalyst-free oxidation was further investigated using NaOH in dimethylformamide (DMF), which produced high FDCA yield (91%) at normal temperature and pressure.<sup>201</sup> The selected system (NaOH in DMF at 25 °C) is the most productive, while changing base (e.g. NaOH with *t*-BuONa or NaH), solvent or any other parameters negatively affects the yield. NaOH-promoted oxidation mechanism of HMF in DMF is outlined in Scheme 18.<sup>201</sup> The influence of the Cannizzaro reaction was observed in the reaction kinetics, which was initiated by a NaOH nucleophilic attack on the aldehyde group, producing the tetrahedral intermediate 2. Intermediate 3 (BHMF) and intermediate 4 (HFCA) were simultaneously



**Scheme 17** Reaction pathway for catalyst-free alkaline medium oxidation of HMF to FDCA using  $\text{H}_2\text{O}_2$ .<sup>199</sup>



**Scheme 18** The reaction mechanism for HMF oxidation promoted by NaOH in DMF.<sup>201</sup>

produced by the migration of the hydride ion from intermediate 2 to another HMF molecule. Intermediate 3 can be quickly oxidized back to HMF. The alcohol group of intermediate 4 was oxidized to the sodium salt of FFCA (intermediate 7) after deprotonation. The aldehyde group present in the sodium salt of FFCA may undergo the Cannizzaro reaction with release of the sodium salt of FDCA (intermediate 8). Due to the solubility difference, FDCA-sodium can be separated *via* acidulation.<sup>201</sup>

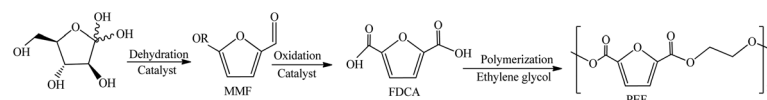
### Industrial process development of FDCA production

The development of the commercial production of FDCA and its derivatives by various industrial ventures in the 21<sup>st</sup> century has indeed been a real breakthrough in the development of biodegradable polymers. The industrial production of FDCA was initiated by Avantium, named the Avantium YXY® process, at the Chemelot campus in Geleen, Holland. The YXY® technology consists of the catalytic dehydration of carbohydrates to alkoxymethylfurfural (RMF) or methoxymethylfurfural (MMF), which is then oxidized to FDCA (Scheme 19). PEF is produced by the catalytic polymerization of FDCA and EG in the last step.<sup>202</sup> The pilot plant started its production in December 2011 with a capacity of 40 tons of FDCA per year. This is the first reported commercial unit for FDCA production.<sup>74</sup> After the successful operation of an FDCA pilot plant, Avantium established a joint venture with BASF (Synvina) and designed a new unit for FDCA production with an extended capacity of 50 000 tons per year with the onsite production of PEF using the same technology.<sup>202</sup> This plant is projected to run in 2023–2024.<sup>74,202</sup> BASF has developed a process using HMF and di-HMF as the substrate for FDCA production in an autoclave over a heterogeneous catalyst.<sup>203,204</sup> Deuterated water ( $D_2O$ ) was used for the preparation of an aqueous solution of HMF and heterogeneous catalyst (Pt) in a molar ratio of 100 : 1 respectively.<sup>203</sup> The autoclave is heated to 185 °C for 20 hours and then cooled to atmospheric temperature for the separation of FDCA solution. Product solution is

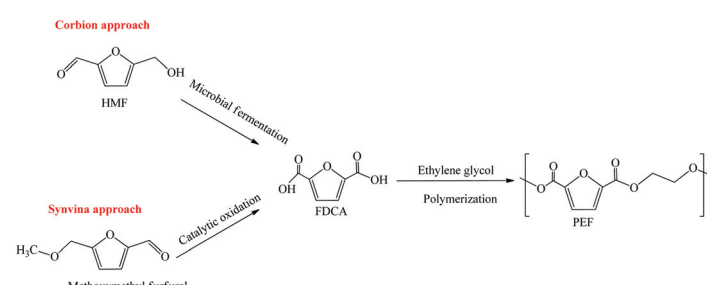
filtered for catalyst separation, and the separated catalyst is washed with water and recycled for subsequent processing.<sup>203</sup> During the oxidation, HMF has the tendency to polymerize, resulting in lower FDCA yield, and this problem can be solved by developing di-HMF oxidation similar to HMF oxidation by BASF. The HMF to di-HMF mass ratio of 1 : 0.5 produced 78.3% of FDCA with complete conversion.<sup>204</sup> The solid catalyst was filtered out from the alkaline solution, washed and recycled.<sup>204</sup> In contrast to the Synvina process, the Corbion process used the microbial route for FDCA production from HMF (Scheme 20).<sup>205</sup> Corbion used highly efficient and selective microbes to develop an industrial process for the large-scale production of FDCA like Succinity® (a joint product of Corbion and BASF), which has efficaciously replaced petroleum-derived succinic acid.<sup>206</sup>

Origin Materials (formerly known as Micromidas) designed the commercial process for the production of FDCA in collaboration with Eastman Chemical Company (Eastman) in 2017.<sup>207</sup> Eastman patented the FDCA production process by the catalytic oxidation of HMF over Co/Mn/Br catalyst with >90% purity (99.2% FDCA yield) in a titanium autoclave (Table 7).<sup>208</sup> The catalyst proportion was maintained using manganese(II) acetate, cobalt(II) acetate tetrahydrate and hydrobromic acid and/or sodium bromide respectively. This production unit will start its operation in the end of 2018 at Western Sarnia-Lambton Research Park.<sup>209</sup>

DuPont Industrial Biosciences (DuPont) in collaboration with Archer Daniels Midland Company (ADM) presented their innovative process to produce 2,5-furandicarboxylic acid dimethyl ester (FDME) in 2016.<sup>210</sup> HMF was oxidized in an aqueous solution of metal salt passing through a high-pressure oxidizer at 115 °C.<sup>211</sup> The pressure increased from 20 bar to 42 bar after 50 minutes of charge. The temperature was maintained at 100 °C for half an hour and then increased to 115–117 °C for 90 minutes (Table 7).<sup>211</sup> The system remained at that pressure for about 15 hours at reduced temperature.



Scheme 19 Process scheme of the Avantium YXY® process for FDCA production.<sup>202</sup>



Scheme 20 The Corbion and Synvina approaches to PEF production.<sup>204,205</sup>

**Table 7** Reported commercial production of FDCA

Research center/company	Substrate	Catalyst	Oxidant	Oxidation environment	Temp. (°C)	Time (h)	Conv. (%)	FDCA yield (%)	Ref.
BASF	HMF	Pt/C (STREM78-1611 Escat2431)	100 Bar air	D <sub>2</sub> O	100	20	100	95.2	203
Synvina (BASF/Avantium)	HMF and di-HMF	Pt/C	100 Bar air	D <sub>2</sub> O	100	18	100 <sup>a</sup>	78.3	204
Eastman/origin materials	HMF	Mn/Co/Br (0.9 : 2 : 3)	8.96 Bar air	Acetic acid	132	2	100	89.4	208
ADM/DuPont	HMF	Metal salt CoBr <sub>2</sub>	42 Bar O <sub>2</sub>	Water solution	115	15	100	40	211
Braskem	Furfural	Au/TiO <sub>2</sub> ; metal salt (CdI <sub>2</sub> /FeCl <sub>2</sub> )	3 Bar O <sub>2</sub>	1.02 equiv. NaOH	265	4	94.9	89	216
NOVAMONT	HMF	Pt/C	5 Bar O <sub>2</sub>	NaHCO <sub>3</sub>	100	4	100	95	218, 219
Petrobras	HMF	Metal catalyst (Pt/Pd/Au)	124 Bar air	NaOH (pH 10–14)	300	—	>90	90	220, 221
VTT	Galactaric acid	Methyl trioxo rhenium	1 Bar air/5 Bar H <sub>2</sub>	MeOH	200	2	60	1.7	224, 225
WARF	HMF	TEMPO (Pt & BiVO <sub>4</sub> electrode)	Electrochemical oxidation	Aqueous boric acid (pH = 9.2)	40	—	99	>90	193, 197

<sup>a</sup> HMF and di-HMF independently.

The produced FDCA was then esterified to produce FDME using an alcoholic mixture under carbon dioxide (CO<sub>2</sub>) atmosphere.<sup>212</sup> This process produces a more stable FDME, which can be then used to produce polytrimethylene furandicarboxylate (PTF) with FDCA.<sup>212</sup> The production facility established at Decatur (Illinois, USA) will start production in 2018.

AVA Biochem, a subsidiary of AVA-CO<sub>2</sub> founded in 2012, successfully started its first manufacturing unit for HMF in 2014 with the hydrothermal processing of biomass and then the production of downstream chemicals from HMF.<sup>213, 214</sup> AVA Biochem has set out to produce FDCA and the first phase will start its production in 2019 with the capacity of 30 000 tons per year, which will be then increased to 120 000 tons per year.<sup>215</sup> This produced FDCA will be used in PEF production by the AVA-CO<sub>2</sub>.<sup>214</sup>

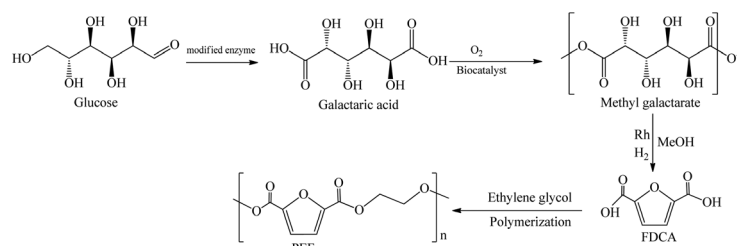
Braskem has developed a process for the catalyzed production of FDCA (2,5-FDCA & 2,4-FDCA) using furfural instead of HMF.<sup>216</sup> Furfural was oxidized to sodium furoate over Au/TiO<sub>2</sub> catalyst in alkaline solution under oxygen pressure (Table 7). Temperature (50 °C) and pressure (3 bar) were maintained overnight with constant stirring.<sup>216</sup> Sodium furoate, after complete mixing with metal salt, was heated to 265 °C for four hours and hydrochloric acid (HCl) was added (pH = 1) for FDCA precipitation. A mixture of 2,5-FDCA & 2,4-FDCA in the proportion of 0.68 : 0.32 was obtained and purified using the acetone/chloroform extraction technique.<sup>216</sup> NOVAMONT developed the process for the production of HMF and FDCA for the captive use of polymer production based on the roots of the cardoon crop (the 5<sup>th</sup> generation MATER-BI®).<sup>217</sup> An aqueous solution of HMF (2% W), catalyst (Pt/C) and sodium bicarbonate (NaHCO<sub>3</sub>) was heated (100 °C) in an autoclave for four hours (Table 7).<sup>218</sup> The required pressure (5 bar) was maintained, regulating the oxygen flow rate (20 l h<sup>-1</sup>). The product mixture was filtered for catalyst recovery and the filtrate was acidified for FDCA precipitation at lower pH.<sup>218</sup> The recovered catalyst, washed

with water and reused, can give 95% FDCA yield in the first two cycles, which is then reduced to 90% in successive cycles.<sup>218, 219</sup>

The two-step FDCA production process was developed by Petrobras.<sup>220, 221</sup> HMF produced from C6 sugars (sucrose, glucose, fructose) in the first step was separated using an ion exchange resin and then converted to FDCA in the second step.<sup>220, 221</sup> Utilization of sub-critical water effectively catalyzed the process and eliminated the additional catalyst requirement (Table 7). A high-pressure oxygen-rich source (air, oxygen etc.) was used with a space velocity of 0.2–4 per hour to achieve the higher yield of FDCA with the maximum conversion of HMF in an integrated process.<sup>220</sup>

VTT Technical Research Centre of Finland Ltd developed an industrial biological process for the production of FDCA from hexanic acid using modified enzymes.<sup>222, 223</sup> The environmentally friendly process used uronate dehydrogenase enzyme (EC 1.1.1.203) for the conversion of D-galacturonic acid into meso-galactaric acid (mucic acid).<sup>224</sup> Typically, galactaric acid was pressurized with hydrogen along with methanol and heated for the production of FDCA over methyl trioxo rhenium catalyst.<sup>225</sup> The production of different furans and muconic acids was dependent upon the process temperature, and 200 °C was optimized for FDCA synthesis (Table 7). The VTT process is differentiated from others by first oxidizing C6 sugars to C6 aldaric acid and then dehydration to FDCA (Scheme 21).<sup>224, 225</sup> Hexanic acid production has been commercialized with economic conversion but the furan production is still under development for commercial production.<sup>222</sup> This method is green, energy efficient and environmentally friendly but has low production volume.

The electrochemical oxidation of HMF using the TEMPO mediator investigated by Choi was further developed by Wisconsin alumni research foundation (WARF) for the industrial production of FDCA (Fig. 3 & Scheme 16).<sup>193, 197</sup> This process has the advantages of high yield, a low-cost electrode



Scheme 21 The VTT process for the production of FDCA.<sup>224,225</sup>

acting as the catalyst, ambient process parameters and higher faradaic efficiency and the utility of photoelectrochemical cells (PECs).<sup>197</sup> Due to these added benefits, WARF is now designing a continuous process for the industrialization of this process with efficient product purification.<sup>226</sup>

The industrial production of FDCA is being developed and has been patented since 2000. Many research and development (R&D) organizations such as Corbion Purac, Mercurius Biorefining,<sup>74,205</sup> and UC Davis, have also developed their processes and are now in the commercial design phase. A summary and comparison of the processes developed and under development are presented in Table 7. As can be seen, early success has been achieved for the commercial production of FDCA with good HMF conversion and FDCA yield; however, the processes are still facing various challenges in terms of product recovery, catalyst recycling, system integration and production cost.

## Conclusion

Biomass-derived FDCA is a promising feedstock for the production of a variety of downstream chemicals. Its most important application is in the production of polymers replacing fossil-derived terephthalic acid (TPA). Therefore, the economical manufacturing of FDCA and its commercialization will not only play a vital role in the production of biodegradable polymers but also reward enormous financial advantages.

Numerous processes for the production of FDCA from HMF or directly from biomass-derived carbohydrates (one-pot synthesis) have been investigated comprehensively in labs and some processes are now growing industrially. These processes include catalytic (both chemical and biological), non-catalytic and electrochemical processes. Due to the high conversion rate and FDCA yield, the chemical-catalytic process emanates as the major FDCA synthesis route. The catalytic processes usually produce a higher yield than non-catalytic processes. Heterogeneous catalytic processes seem to be more promising than homogenous catalytic processes because of the associated merits such as easy separation of product and good recyclability of the catalyst. The most used catalysts are oxides of noble metals; however, their high cost, poor availability and recyclability are the major hindrances to their commercial acceptance. Transition metal oxides are good alternatives but

suffer from low FDCA yield. However, these catalysts are associated with the benefits of heterogeneous catalysis together with low cost and availability, and hence are good candidates for industrialization.

Molecular oxygen is the most promising oxidant for oxidation of HMF to FDCA because of its availability and relatively low cost, but high-pressure is usually required. Researchers have devoted their efforts to the commercial design of the catalytic aerobic oxidative production of FDCA from HMF utilizing noble metal catalysts. Particle size, support, and the active phase play vital roles in the catalytic activity, together with process conditions such as temperature, pressure, flow rate and oxygen pressure. In term of the stability, Au-based catalysts are more selective than Pd and Pt-based catalysts due to their stability in the oxidizing environment. Deactivation of the metal-based catalysts with process intermediates and by-products results in reduced catalytic activity in successive cycles. Alloying of Pd, Cu or Pt with a Au-based catalyst to produce a bimetallic catalyst can impressively upgrade the catalytic activity and selectivity. HFCA was detected as a process intermediate during the Au metal-based alkaline medium oxidation, whereas base-free oxidation proceeded *via* the DFF route. This phenomenon strongly suggests that aldehyde group oxidation in HMF is faster than alcohol group oxidation in basic medium. Isotope labeling technology has revealed that the reaction mechanism is the same both in basic and base-free environments. The oxygen that is merged into the HMF structure to yield FDCA is incorporated from water molecules rather than the oxidizing agent (molecular oxygen) available in the system. Molecular oxygen only plays a role in catalyst reimbursement by replacing electron deposition in the supported metal particles.

Fructose is mostly used for the direct conversion of carbohydrates to FDCA in a one-pot process, but the one-pot one-step process just gives a low FDCA yield, and the development of the one-pot two-step process has increased the yield to some extent but the yield is not yet competitive. The one-pot process is more encouraging for FDCA synthesis due to HMF instability, poor availability and potential economics. Improvement in technology can make this process more cost-effective and feasible by excluding the barrier of HMF extraction and purification.

Different electrochemical processes have been investigated for the production of FDCA with the additional advantage of

clean H<sub>2</sub> production but the yield is very low. The yield can be improved by employing more stable and active electrocatalysts. Electrochemical oxidation of HMF can be a good alternative route for FDCA production with simultaneous H<sub>2</sub> production, which will serve as a green source of energy. Biocatalytic processes can produce FDCA with comparative yields under mild conditions. However, low HMF concentration in comparison to that of metal oxide catalysis is the primary barrier for the practical application of the biological route.

Industrial production of FDCA is being vigorously developed, and early success has been made with good HMF conversion and FDCA yield. Most of the developed processes with commercial potential are based on chemical-catalytic routes with metal catalysts; however, there are still various challenges in terms of product recovery, catalyst recycling, system integration and production cost.

## Future prospective

Substantial work has been done for the production of FDCA from different bioresources with numerous catalysts, techniques and environments. However, in spite of numerous lab-scale processes, there is still no well-established market share of FDCA in the polymer market. Actually, HMF has an equal or sometimes even higher price than FDCA, so the question arises as to why produce FDCA. Further developments are still required in oxidation methodologies for mass production in view of industrialization and commercial economics. Based upon this review, the following directions for future research and development are recommended:

(1) Extensive evaluation and correlation of different catalysts for the catalyzed oxidation of HMF to FDCA will help in process selection. Heterogeneous catalysts in comparison to homogeneous catalysts and catalyst-free models are more promising due to separation and recycling efficiencies. Non-noble metal catalysts in contrast to noble metal catalysts are not widely focused on. Transition metal catalysts are an economical industrial alternative because of their cost, availability, and stability. Bimetallic catalysts (a combination of noble and non-noble metals) are also promising substitutes with improved catalytic ability and stability as compared to a mono-metallic catalyst. Alloying with other metals such as copper or palladium boosts FDCA selectivity with extended recyclability and stability. A comprehensive comparison of catalytic efficiency, stability, and the cost of these catalysts for application in FDCA production will increase the catalyst selectivity and catalyst development methodologies. Further work in transition metal catalyst and bimetallic catalysts will be more imperative.

(2) Noble metal heterogeneous catalysts still suffer from instability and degradation problems. Different techniques such as cage encapsulated nanoparticles, CNT structure and increased interaction between metallic particles and support can avoid agglomeration, thus improving the catalyst stability and reactivity. Using alloying techniques (either bimetallic or

trimetallic) will further improve the catalytic activity and stability. However, the design of the catalyst and supports, combined with molecular simulation, may provide new insights to guide the process.

(3) Experiments performed in alkaline solution make the process expensive and less green. Additionally, FDCA salt neutralization increases the operating cost and time with additional by-product formation. Base-free systems suffer from low yield and selectivity and, therefore, have not been researched extensively. As such extensive work is required to develop a catalyst focusing on base-free conversion systems with extended reactivity.

(4) The utilization of LCB fractions (cellulose, glucose, and fructose) for the one-pot production of FDCA can eliminate the HMF separation and instability problems. Direct utilization of these fractions will improve the economic feasibility with optimized production technologies, as these are cheaply and abundantly available. Designing a multifunctional catalyst with the combined effect of acid, base and metal sites will definitely achieve this goal. The placement of acid/base sites in the hydrophilic environment for carbohydrate dehydration to HMF, and metal sites in the hydrophobic environment for oxidation of HMF to FDCA are suggested. This will improve carbohydrate absorbance on acid/base sites and HMF will desorb quickly toward hydrophobic metal sites for oxidation. This scheme will improve the overall yield and selectivity. However, how to efficiently and economically release glucose from LCB should be considered.

(5) Ionic liquids and deep eutectic solvents with their multifunctionalities and acid-base properties are in continuous development. The merger of the reaction chemistry of direct conversions of fructose to FDCA with the solvents having catalytic behavior will extend their utilization in one-pot synthesis. These systems have reactive solvent properties but environmental concerns need to be addressed for their commercial utilization.

(6) The chemical kinetics and reaction mechanism of FDCA production either from HMF oxidation or directly from sugars have not been extensively studied. An in-depth understanding of the reaction mechanism will facilitate the rational design of robust, economical and efficient catalysts with extended life and efficient recycling.

(7) Last but not least, the mass production of FDCA is exceptionally important for the establishment of a green environment. Many developed methods are technologically viable but financially exorbitant. Optimized process design is a long-lasting challenge for researchers. The approach of interdisciplinary research, involving material engineering, chemistry, and process design, may achieve this objective and improve the process.

## Conflicts of interest

There are no conflicts to declare.

## Acknowledgements

Authors are grateful to the supports of this work by National Natural Science Foundation of China (No. 21878176) and National Energy Administration Project of China (No. NY20130402).

## References

- 1 R. A. Sheldon, *Green Chem.*, 2014, **16**, 950–963.
- 2 D. A. Bulushev and J. R. H. Ross, *ChemSusChem*, 2018, **11**, 821–836.
- 3 A. Corma, A. Sara Iborra and A. Velty, *Chem. Rev.*, 2007, **107**(6), 2411–2502.
- 4 P. Gallezot, *Chem. Soc. Rev.*, 2012, **41**, 1538–1558.
- 5 R. D. Perlack, L. L. Wright, A. F. Turhollow, R. L. Graham, B. J. Stokes and D. C. Erbach, *Agriculture*, 2005, **DOE-GO-102**, 78.
- 6 S. Roy Goswami, M. J. Dumont and V. Raghavan, *Starch*, 2016, **68**, 274–286.
- 7 E. Article, L. Ardemani, G. Cibin, A. J. Dent, M. A. Isaacs, G. Kyriakou, A. F. Lee, C. M. A. Parlett and A. Parry, *Chem. Sci.*, 2015, **6**, 4940–4945.
- 8 I. Delidovich, P. J. C. Hausoul, L. Deng, R. Pfützenreuter, M. Rose and R. Palkovits, *Chem. Rev.*, 2016, **116**, 1540–1599.
- 9 X. Tang, M. Zuo, Z. Li, H. Liu, C. Xiong, X. Zeng, Y. Sun, L. Hu, S. Liu, T. Lei and L. Lin, *ChemSusChem*, 2017, **10**, 2696–2706.
- 10 J. Zhang, L. Lin and S. Liu, *Energy Fuels*, 2012, **26**, 4560–4567.
- 11 R. D. Perlack, B. J. Stokes, L. M. Eaton and A. F. Turnhollow, *Renewable Energy*, 2005, **7**, 1–229.
- 12 H. Ohara, *Appl. Microbiol. Biotechnol.*, 2003, **62**, 474–477.
- 13 K. M. Zia, A. Noreen, M. Zuber, S. Tabasum and M. Mujahid, *Int. J. Biol. Macromol.*, 2016, **82**, 1028–1040.
- 14 S. Marques, A. D. Moreno, M. Ballesteros and F. Gírio, in *Biomass and Green Chemistry*, Springer International Publishing, Cham, 2018, pp. 69–94.
- 15 Z. Jia, J. Wang, L. Sun, J. Zhu and X. Liu, *J. Appl. Polym. Sci.*, 2018, **135**, 46076.
- 16 X. Tong, S. Xue and J. Hu, *Production of Platform Chemicals from Sustainable Resources*, 2017.
- 17 M. Brodin, M. Vallejos, M. T. Opdal, M. C. Area and G. Chinga-Carrasco, *J. Cleaner Prod.*, 2017, **162**, 646–664.
- 18 R. Moscoviz, E. Trably, N. Bernet and H. Carrère, *Green Chem.*, 2018, **20**, 3159–3179.
- 19 L. Axelsson, M. Franzén, M. Ostwald, G. Berndes, G. Lakshmi and N. H. Ravindranath, *Biofuels, Bioprod. Bioref.*, 2012, **6**, 246–256.
- 20 H. Kobayashi and A. Fukuoka, *Green Chem.*, 2013, **15**, 1740.
- 21 S. Morales-delaRosa, J. M. Campos-Martin and J. L. G. Fierro, *Cellulose*, 2014, **21**, 2397–2407.
- 22 S. Van de Vyver, J. Geboers, P. A. Jacobs and B. F. Sels, *ChemCatChem*, 2011, **3**, 82–94.
- 23 W. Li, T. Zhang, H. Xin, M. Su, L. Ma, H. Jameel, H. Chang and G. Pei, *RSC Adv.*, 2017, **7**, 27682–27688.
- 24 S. Zhu, J. Wang and W. Fan, *Catal. Sci. Technol.*, 2015, **5**, 3845–3858.
- 25 B. Girisuta and H. J. Heeres, *Levulinic Acid from Biomass: Synthesis and Applications*, Springer, Singapore, 2017, pp. 143–169.
- 26 M. Saif Ur Rehman, I. Kim, N. Rashid, M. Adeel Umer, M. Sajid and J. I. Han, *Clean: Soil, Air, Water*, 2016, **44**, 55–62.
- 27 Y. Zhang, A. Kumar, P. R. Hardwidge, T. Tanaka, A. Kondo and P. V. Vadlani, *Biotechnol. Prog.*, 2016, **32**, 271–278.
- 28 C. Marques, R. Tarek, M. Sara and S. K. Brar, in *Platform Chemical Biorefinery*, Elsevier, 2016, pp. 217–227.
- 29 C.-H. Zhou, X. Xia, C.-X. Lin, D.-S. Tong and J. Beltramini, *Chem. Soc. Rev.*, 2011, **40**, 5588.
- 30 X. Cui, X. Zhao and D. Liu, *Green Chem.*, 2018, **20**, 2018–2026.
- 31 J. Song, H. Fan, J. Ma and B. Han, *Green Chem.*, 2013, **15**, 2619.
- 32 P. L. Dhepe and R. Sahu, *Green Chem.*, 2010, **12**, 2153.
- 33 F. Peng, J. L. Ren, F. Xu and R. Sun, *Sustainable Prod. Fuels, Chem. Fibers For. Biomass*, 2011, 219–259.
- 34 C. Xu, R. A. D. Arancon, J. Labidi and R. Luque, *Chem. Soc. Rev.*, 2014, **43**, 7485–7500.
- 35 S. Zhang, T. Liu, C. Hao, L. Wang, J. Han, H. Liu and J. Zhang, *Green Chem.*, 2018, **20**, 2995–3000.
- 36 A. R. C. Morais, A. M. da Costa Lopes and R. Bogel-Lukasik, *Chem. Rev.*, 2015, **115**, 3–27.
- 37 C. S. Lancefield, L. W. Teunissen, B. M. Weckhuysen and P. C. A. Bruijnincx, *Green Chem.*, 2018, **20**, 3214–3221.
- 38 L. Ardemani, G. Cibin, A. J. Dent, M. A. Isaacs, G. Kyriakou, A. F. Lee, C. M. A. Parlett, S. A. Parry and K. Wilson, *Chem. Sci.*, 2015, **6**, 4940–4945.
- 39 E. De Jong, M. A. Dam and L. Sipos, Furandicarboxylic Acid (FDCA), A Versatile Building Block for a Very Interesting Class of Polyesters, in *Biobased Monomers, Polymers, and Materials*, American Chemical Society, 2012, DOI: 10.1021/bk-2012-1105.ch001, ISBN: 9780841227675.
- 40 Z. Zhang and G. W. Huber, *Chem. Soc. Rev.*, 2018, **47**, 1351–1390.
- 41 E. De Jong, M. A. Dam, L. Sipos and G.-J. M. Gruter, in *Biobased Monomers, Polymers, and Materials*, ed. American Chemical Society, Copyright © 2012 American Chemical Society, Avantium Chemicals BV, Zekeringstraat 29, 1014 BV Amsterdam, The Netherlands, 2012, vol. 1105, pp. 1–13.
- 42 T. Pan, J. Deng, Q. Xu, Y. Zuo, Q. X. Guo and Y. Fu, *ChemSusChem*, 2013, **6**, 47–50.
- 43 S. H. Swan, *Environ. Res.*, 2008, **108**, 177–184.
- 44 M.-Y. Chen, M. Ike and M. Fujita, *Environ. Toxicol.*, 2002, **17**, 80–86.
- 45 G. L. Ball, C. J. McLellan and V. S. Bhat, *Crit. Rev. Toxicol.*, 2012, **42**, 28–67.
- 46 A. J. J. E. Eerhart, A. P. C. Faaij and M. K. Patel, *Energy Environ. Sci.*, 2012, **5**, 6407.

- 47 G. Chen, N. M. Van Straalen and D. Roelofs, *Green Chem.*, 2016, **18**, 4420–4431.
- 48 X.-X. Zhang, S.-L. Sun, Y. Zhang, B. Wu, Z.-Y. Zhang, B. Liu, L.-Y. Yang and S.-P. Cheng, *J. Hazard. Mater.*, 2010, **176**, 300–305.
- 49 T. J. Schwartz, B. J. O'Neill, B. H. Shanks and J. A. Dumesic, *ACS Catal.*, 2014, **4**, 2060–2069.
- 50 M. Ambia and S. Salehi, *Chem. Eng. Res. Des.*, 2012, **90**, 975–983.
- 51 L. Niu, Y. Xu, C. Xu, L. Yun and W. Liu, *Environ. Pollut.*, 2014, **195**, 16–23.
- 52 A. F. Sousa, C. Vilela, A. C. Fonseca, M. Matos, C. S. R. Freire, G.-J. M. Gruter, J. F. J. Coelho and A. J. D. Silvestre, *Polym. Chem.*, 2015, **6**, 5961–5983.
- 53 R. Auvergne, S. Caillol, G. David, B. Boutevin and J.-P. Pascault, *Chem. Rev.*, 2014, **114**, 1082–1115.
- 54 P. H. Witten, T. A. Levine, S. P. Killan and M. Boyle, *S. Clin. Chem.*, 1973, **19**, 575t.
- 55 K. Koide, J. Toyama, N. Inoue, S. Koshikawa, T. Akizawa and K. Takahashi, *Chem. Abstr.*, 1987, **106**, 192091g.
- 56 D. T. Richter and T. D. Lash, *Tetrahedron Lett.*, 1999, **40**, 6735–6738.
- 57 M. Del Poeta, W. A. Schell, C. C. Dykstra, S. Jones, R. R. Tidwell, A. Czarny, M. Bajic, A. Kumar, D. Boykin and J. R. Perfect, *Antimicrob. Agents Chemother.*, 1998, **42**, 2495–2502.
- 58 M. Grass and H. G. Becker, *US Pat.*, 20120202725A1, Evonik Oxeno GmbH, 2012.
- 59 M. Grass and H. G. Becker, *WO Pat.*, 2011023590A1, Evonik Oxeno GmbH, 2011.
- 60 H. G. Becker and M. Grass, *WO Pat.*, 2012113608A1, Evonik Oxeno GmbH, 2012.
- 61 H. G. Becker, M. Grass, A. Huber and M. Woelk-Faehrmann, *WO Pat.*, WO2012113609A1, Evonik Oxeno GmbH, 2012.
- 62 D. B. Larsen, R. Sønderbæk-Jørgensen, J. Ø. Duus and A. E. Daugaard, *Eur. Polym. J.*, 2018, **102**, 1–8.
- 63 M. J. Gilkey, R. Balakumar, D. G. Vlachos and B. Xu, *Catal. Sci. Technol.*, 2018, **8**, 2661–2671.
- 64 O. W. Howarth, G. G. Morgan, V. McKee and J. Nelson, *J. Chem. Soc., Dalton Trans.*, 1999, 2097–2102.
- 65 A. F. Sousa, C. Vilela, A. C. Fonseca, M. Matos, C. S. R. Freire, G.-J. M. Gruter, J. F. J. Coelho and A. J. D. Silvestre, *Polym. Chem.*, 2015, **6**, 5961–5983.
- 66 J. J. Pacheco and M. E. Davis, *Proc. Natl. Acad. Sci. U. S. A.*, 2014, **111**, 8363–8367.
- 67 D. Yan, J. Xin, Q. Zhao, K. Gao, X. Lu, G. Wang and S. Zhang, *Catal. Sci. Technol.*, 2018, **8**, 164–175.
- 68 D. I. Collias, A. M. Harris, V. Nagpal, I. W. Cottrell and M. W. Schultheis, *Ind. Biotechnol.*, 2014, **10**, 91–105.
- 69 J. Tomaszewska, D. Bieliński, M. Binczarski, J. Berlowska, P. Dziugan, J. Piotrowski, A. Stanishevsky and I. A. Witońska, *RSC Adv.*, 2018, **8**, 3161–3177.
- 70 S. Matsumura, A. R. Hlil, C. Lepiller, J. Gaudet, D. Guay, Z. Shi, S. Holdcroft and A. S. Hay, *Am. Chem. Soc. Polym. Prepr. Div. Polym. Chem.*, 2008, **49**, 511–512.
- 71 A. Kasai and S. Kato, *JP Pat.*, 2008291244, Mitsubishi Chemicals Corp, 2008.
- 72 S. K. Burgess, J. E. Leisen, B. E. Kraftschik, C. R. Mubarak, R. M. Kriegel and W. J. Koros, *Macromolecules*, 2014, **47**, 1383–1391.
- 73 G. Z. Papageorgiou, D. G. Papageorgiou, Z. Terzopoulou and D. N. Bikaris, *Eur. Polym. J.*, 2016, **83**, 202–229.
- 74 Biorefineries of FDCA, <https://biorrefineria.blogspot.com/2017/06/biorefinerias-de-fdca-acido-2-5-furanodicarboxilico-PEF.html> (accessed 21 September 2018).
- 75 J. Lewkowski, *ARKIVOC*, 2001, 17–54.
- 76 K. F. Wang, C. L. Liu, K. Y. Sui, C. Guo and C. Z. Liu, *ChemBioChem*, 2018, **19**, 654–659.
- 77 Z. Zhang, J. Zhen, B. Liu, K. Lv and K. Deng, *Green Chem.*, 2015, **17**, 1308–1317.
- 78 A. Karich, S. Kleeberg, R. Ullrich and M. Hofrichter, *Microorganisms*, 2018, **6**, 5.
- 79 M. Tan, L. Ma, M. S. U. Rehman, M. A. Ahmed, M. Sajid, X. Xu, Y. Sun, P. Cui and J. Xu, *Renewable Energy*, 2019, **132**, 950–958.
- 80 D. J. Chadderdon, L. Xin, J. Qi, Y. Qiu, P. Krishna, K. L. More and W. Li, *Green Chem.*, 2014, **16**, 3778–3786.
- 81 H. Fittig and R. Heinzelmann, *Chem. Ber.*, 1876, 1198.
- 82 M. Rose, D. Weber, B. V. Lotsch, R. K. Kremer, R. Goddard and R. Palkovits, *Microporous Mesoporous Mater.*, 2013, **181**, 217–221.
- 83 G. Gonis and E. D. Amstutz, *J. Org. Chem.*, 1962, **27**, 2946–2947.
- 84 Y. Xuan, R. He, B. Han, T. Wu and Y. Wu, *Waste Biomass Valorization*, 2018, **9**, 401–408.
- 85 D. Yan, J. Xin, Q. Zhao, K. Gao, X. Lu, G. Wang and S. Zhang, *Catal. Sci. Technol.*, 2018, **8**, 164–175.
- 86 W. P. Dijkman, D. E. Groothuis and M. W. Fraaije, *Angew. Chem., Int. Ed.*, 2014, **53**, 6515–6518.
- 87 D.-H. Nam, B. J. Taitt and K.-S. Choi, *ACS Catal.*, 2018, **8**, 1197–1206.
- 88 Z. Zhang and K. Deng, *ACS Catal.*, 2015, **5**, 6529–6544.
- 89 C.-T. Chen, C. Van Nguyen, Z.-Y. Wang, Y. Bando, Y. Yamauchi, M. T. S. Bazziz, A. Fatehmulla, W. A. Farooq, T. Yoshikawa, T. Masuda and K. C.-W. Wu, *ChemCatChem*, 2018, **10**, 361–365.
- 90 H. Ban, T. Pan, Y. Cheng, L. Wang and X. Li, *J. Chem. Eng. Data*, 2018, **63**, 1987–1993.
- 91 W. Partenheimer and V. V. Grushin, *Adv. Synth. Catal.*, 2001, **343**, 102–111.
- 92 A. Z. Fadhel, P. Pollet, C. L. Liotta and C. A. Eckert, *Molecules*, 2010, **15**, 8400–8424.
- 93 P. Verdeguer, N. Merat and A. Gaset, *J. Mol. Catal.*, 1993, **85**, 327–344.
- 94 H. Ait Rass, N. Essayem and M. Besson, *Green Chem.*, 2013, **15**, 2240.
- 95 S. E. Davis, L. R. Houk, E. C. Tamargo, A. K. Datye and R. J. Davis, *Catal. Today*, 2011, **160**, 55–60.

- 96 K. R. Vuyyuru and P. Strasser, *Catal. Today*, 2012, **195**, 144–154.
- 97 H. Ait Rass, N. Essayem and M. Besson, *ChemSusChem*, 2015, **8**, 1206–1217.
- 98 W. Niu, D. Wang, G. Yang, J. Sun, M. Wu, Y. Yoneyama and N. Tsubaki, *Bull. Chem. Soc. Jpn.*, 2014, **87**, 1124–1129.
- 99 P. Vinke, H. E. van Dam and H. van Bekkum, *Stud. Surf. Sci. Catal.*, 1990, **55**, 147–158.
- 100 R. Sahu and P. L. Dhepe, *React. Kinet., Mech. Catal.*, 2014, **112**, 173–187.
- 101 H. Chen, J. Shen, K. Chen, Y. Qin, X. Lu, P. Ouyang and J. Fu, *Appl. Catal., A*, 2018, **555**, 98–107.
- 102 Z. Miao, T. Wu, J. Li, T. Yi, Y. Zhang and X. Yang, *RSC Adv.*, 2015, **5**, 19823–19829.
- 103 S. Siankevich, G. Savoglidis, Z. Fei, G. Laurenczy, D. T. L. Alexander, N. Yan and P. J. Dyson, *J. Catal.*, 2014, **315**, 67–74.
- 104 Y. Zhang, Z. Xue, J. Wang, X. Zhao, Y. Deng, W. Zhao and T. Mu, *RSC Adv.*, 2016, **6**, 51229–51237.
- 105 S. Siankevich, S. Mozzettini, F. Bobbink, S. Ding, Z. Fei, N. Yan and P. J. Dyson, *ChemPlusChem*, 2018, **83**, 19–23.
- 106 H. V. Inke, P. Poel and W. V. Bikkum, *Studies in Surface Science and Catalysis*, Elsevier, Amsterdam, 1991.
- 107 A. H. Motagamwala, W. Won, C. Sener, D. M. Alonso, C. T. Maravelias, J. A. Dumesic, A. Hussain Motagamwala, W. Won, C. Sener, D. M. Alonso, C. T. Maravelias and J. A. Dumesic, *Sci. Adv.*, 2018, **4**, eaap9722.
- 108 N. Yan, Y. Yuan and P. J. Dyson, *Dalton Trans.*, 2013, **42**, 13294.
- 109 B. Siyo, M. Schneider, M.-M. Pohl, P. Langer and N. Steinfeldt, *Catal. Lett.*, 2014, **144**, 498–506.
- 110 B. Siyo, M. Schneider, J. J. Radnik, M.-M. M. Pohl, P. Langer and N. Steinfeldt, *Appl. Catal., A*, 2014, **478**, 107–116.
- 111 B. Liu, Y. Ren and Z. Zhang, *Green Chem.*, 2015, **17**, 1610–1617.
- 112 N. Mei, B. Liu, J. Zheng, K. Lv, D. Tang and Z. Zhang, *Catal. Sci. Technol.*, 2015, **5**, 3194–3202.
- 113 H. Xia, J. An, M. Hong, S. Xu, L. Zhang and S. Zuo, *Catal. Today*, 2019, **319**(1), 113–120.
- 114 A. Lolli, S. Albonetti, L. Utili, R. Amadori, F. Ospitali, C. Lucarelli and F. Cavani, *Appl. Catal., A*, 2015, **504**, 408–419.
- 115 Y. Wang, K. Yu, D. Lei, W. Si, Y. Feng, L.-L. Lou and S. Liu, *ACS Sustainable Chem. Eng.*, 2016, **4**, 4752–4761.
- 116 P. V. Rathod and V. H. Jadhav, *ACS Sustainable Chem. Eng.*, 2018, **6**, 5766–5771.
- 117 G. J. Hutchings, *J. Catal.*, 1985, **96**, 292–295.
- 118 M. Haruta, T. Kobayashi, H. Sano and N. Yamada, *Chem. Lett.*, 1987, **16**, 405–408.
- 119 M. Pan, A. J. Brush, Z. D. Pozun, H. C. Ham, W.-Y. Yu, G. Henkelman, G. S. Hwang and C. B. Mullins, *Chem. Soc. Rev.*, 2013, **42**, 5002.
- 120 A. Wittstock, A. Wichmann and M. Bäumer, *ACS Catal.*, 2012, **2**, 2199–2215.
- 121 O. Casanova, S. Iborra and A. Corma, *ChemSusChem*, 2009, **2**, 1138–1144.
- 122 S. Albonetti, A. Lolli, V. Morandi, A. Migliori, C. Lucarelli and F. Cavani, *Appl. Catal., B*, 2015, **163**, 520–530.
- 123 Z. Miao, Y. Zhang, X. Pan, T. Wu, B. Zhang, J. Li, T. Yi, Z. Zhang and X. Yang, *Catal. Sci. Technol.*, 2015, **5**, 1314–1322.
- 124 J. Cai, H. Ma, J. Zhang, Q. Song, Z. Du, Y. Huang and J. Xu, *Chem. – Eur. J.*, 2013, **19**, 14215–14223.
- 125 Y. Y. Gorbanev, S. K. Klitgaard, J. M. Woodley, C. H. Christensen and A. Riisager, *ChemSusChem*, 2009, **2**, 672–675.
- 126 M. Kim, Y. Su, A. Fukuoka, E. J. M. Hensen and K. Nakajima, *Angew. Chemie*, 2018, **130**(27), 8367–8371.
- 127 Y. Wu, D. Wang, G. Zhou, R. Yu, C. Chen and Y. Li, *J. Am. Chem. Soc.*, 2014, **136**, 11594–11597.
- 128 S. Rasul, D. H. Anjum, A. Jedidi, Y. Minenkov, L. Cavallo and K. Takanabe, *Angew. Chem., Int. Ed.*, 2015, **54**, 2146–2150.
- 129 T. Pasini, M. Piccinini, M. Blosi, R. Bonelli, S. Albonetti, N. Dimitratos, J. A. Lopez-Sánchez, M. Sankar, Q. He, C. J. Kiely, G. J. Hutchings and F. Cavani, *Green Chem.*, 2011, **13**, 2091.
- 130 S. Albonetti, T. Pasini, A. Lolli, M. Blosi, M. Piccinini, N. Dimitratos, J. A. Lopez-Sánchez, D. J. Morgan, A. F. Carley, G. J. Hutchings and F. Cavani, *Catal. Today*, 2012, **195**, 120–126.
- 131 A. Villa, M. Schiavoni, S. Campisi, G. M. Veith and L. Prati, *ChemSusChem*, 2013, **6**, 609–612.
- 132 X. Wan, C. Zhou, J. Chen, W. Deng, Q. Zhang, Y. Yang and Y. Wang, *ACS Catal.*, 2014, **4**, 2175–2185.
- 133 N. K. Gupta, S. Nishimura, A. Takagaki and K. Ebitani, *Green Chem.*, 2011, **13**, 824.
- 134 B. N. Zope, S. E. Davis and R. J. Davis, *Top. Catal.*, 2012, **55**, 24–32.
- 135 A. Lolli, R. Amadori, C. Lucarelli, M. G. Cutrufello, E. Rombi, F. Cavani and S. Albonetti, *Microporous Mesoporous Mater.*, 2016, **226**, 466–475.
- 136 M. E. Zakrzewska, E. Bogel-Łukasik and R. Bogel-Łukasik, *Chem. Rev.*, 2011, **111**, 397–417.
- 137 J. Artz, S. Mallmann and R. Palkovits, *ChemSusChem*, 2015, **8**, 672–679.
- 138 J. Nie, J. Xie and H. Liu, *J. Catal.*, 2013, **301**, 83–91.
- 139 S. Wang, Z. Zhang, B. Liu and J. Li, *Ind. Eng. Chem. Res.*, 2014, **53**, 5820–5827.
- 140 Y. Y. Gorbanev, S. Kegnæs and A. Riisager, *Top. Catal.*, 2011, **54**, 1318–1324.
- 141 Y. Y. Gorbanev, S. Kegnæs and A. Riisager, *Catal. Lett.*, 2011, **141**, 1752–1760.
- 142 G. Yi, S. P. Teong and Y. Zhang, *Green Chem.*, 2016, **18**, 979–983.
- 143 T. Ståhlberg, E. Eyjólfssdóttir, Y. Y. Gorbanev, I. Sádaba and A. Riisager, *Catal. Lett.*, 2012, **142**, 1089–1097.
- 144 D. K. Mishra, H. J. Lee, J. Kim, H.-S. Lee, J. K. Cho, Y.-W. Suh, Y. Yi and Y. J. Kim, *Green Chem.*, 2017, **19**, 1619–1623.

- 145 C. M. Pichler, M. G. Al-Shaal, D. Gu, H. Joshi, W. Ciptonugroho and F. Schüth, *ChemSusChem*, 2018, **11**(13), 2083–2090.
- 146 T. Gao, Y. Yin, W. Fang and Q. Cao, *Mol. Catal.*, 2018, **450**, 55–64.
- 147 J. Van Krieken and A. B. De Haan, *US* 2018/0044312A1, 2018.
- 148 F. Kerdi, H. Ait Rass, C. Pinel, M. Besson, G. Peru, B. Leger, S. Rio, E. Monflier and A. Ponchel, *Appl. Catal., A*, 2015, **506**, 206–219.
- 149 B. Saha, D. Gupta, M. M. Abu-Omar, A. Modak and A. Bhaumik, *J. Catal.*, 2013, **299**, 316–320.
- 150 L. Gao, K. Deng, J. Zheng, B. Liu and Z. Zhang, *Chem. Eng. J.*, 2015, **270**, 444–449.
- 151 A. Jain, S. C. Jonnalagadda, K. V. Ramanujachary, A. Mugweru, A. Manuscript, A. Jain, S. C. Jonnalagadda, K. V. Ramanujachary and A. Mugweru, *CATCOM*, 2015, **58**, 179–182.
- 152 S. Wang, Z. Zhang and B. Liu, *ACS Sustainable Chem. Eng.*, 2015, **3**, 406–412.
- 153 F. Neațu, R. S. Marin, M. Florea, N. Petrea, O. D. Pavel, V. I. Pârvulescu, F. Neațu, R. S. Marin, M. Florea, N. Petrea, O. D. Pavel and V. I. Pârvulescu, *Appl. Catal., B*, 2016, **180**, 751–757.
- 154 D. Yan, J. Xin, C. Shi, X. Lu, L. Ni, G. Wang and S. Zhang, *Chem. Eng. J.*, 2017, **323**, 473–482.
- 155 S. Zhang, X. Sun, Z. Zheng and L. Zhang, *Catal. Commun.*, 2018, **113**, 19–22.
- 156 A. Stark, M. Wild, M. Ramzan, M. M. Azim and A. Schmidt, in *Product Design and Engineering*, ed. U. Brockel, W. Meier and G. Wagner, Wiley - VCH, Singapore, 1st edn, 2007, pp. 169–210.
- 157 C. Florindo, L. Romero, I. Rintoul, L. C. Branco and I. M. Marrucho, *ACS Sustainable Chem. Eng.*, 2018, **6**, 3888–3895.
- 158 E. L. Smith, A. P. Abbott and K. S. Ryder, *Chem. Rev.*, 2014, **114**, 11060–11082.
- 159 Y.-Z. Qin, Y.-M. Li, M.-H. Zong, H. Wu and N. Li, *Green Chem.*, 2015, **17**, 3718–3722.
- 160 S. E. Davis, B. N. Zope and R. J. Davis, *Green Chem.*, 2012, **14**, 143–147.
- 161 S. E. Davis, A. D. Benavidez, R. W. Gosselink, J. H. Bitter, K. P. de Jong, A. K. Datye and R. J. Davis, *J. Mol. Catal. A: Chem.*, 2014, **388–389**, 123–132.
- 162 J. Lewkowski, *Gen. Pap. Ark.*, 2001, 17–54.
- 163 E. Slavinskaya, V. A. Kreile, D. R. Dziluma, E. Eglite, D. Milmanis, I. Korchogova, U. Kh. Avots and A. Pinka, *Chem. Abstr.*, 1978, 146670c.
- 164 B. N. Zope, D. D. Hibbitts, M. Neurock and R. J. Davis, *Science*, 2010, **330**, 74–78.
- 165 C. V. Nguyen, Y.-T. Liao, T.-C. Kang, J. E. Chen, T. Yoshikawa, Y. Nakasaka, T. Masuda and K. C.-W. Wu, *Green Chem.*, 2016, **18**, 5957–5961.
- 166 A. Mukherjee, M.-J. J. Dumont and V. Raghavan, *Biomass Bioenergy*, 2015, **72**, 143–183.
- 167 I. K. M. Yu and D. C. W. Tsang, *Bioresour. Technol.*, 2017, **238**, 716–732.
- 168 S. Kowalski, M. Lukasiewicz, A. Duda-Chodak and G. Zięć, *Pol. J. Food Nutr. Sci.*, 2013, **63**, 207–225.
- 169 A. A. Rosatella, S. P. Simeonov, R. F. M. Frade and C. A. M. Afonso, *Green Chem.*, 2011, **13**, 754.
- 170 A. Cadu, K. Sekine, J. Mormul, D. M. Ohlmann, T. Schaub and A. S. K. Hashmi, *Green Chem.*, 2018, **20**, 3386–3393.
- 171 F. H. Isikgor and C. R. Becer, *Polym. Chem.*, 2015, **6**, 4497–4559.
- 172 M. Kröger, U. Prüß and K. Vorlop, *Top. Catal.*, 2000, **13**, 237–242.
- 173 B. Saha and M. M. Abu-Omar, *Green Chem.*, 2014, **16**, 24–38.
- 174 M. L. Ribeiro and U. Schuchardt, *Catal. Commun.*, 2003, **4**, 83–86.
- 175 G. Yi, S. P. Teong, X. Li, Y. Zhang, S. Ping Teong, X. Li, Y. Zhang, S. P. Teong, X. Li and Y. Zhang, *ChemSusChem*, 2014, **7**, 2131–2135.
- 176 S. P. Teong, G. Yi, X. Cao and Y. Zhang, *ChemSusChem*, 2014, **7**, 2120–2124.
- 177 G. Yi, S. P. Teong and Y. Zhang, *ChemSusChem*, 2015, **8**, 1151–1155.
- 178 S. Wang, Z. Zhang and B. Liu, *ACS Sustainable Chem. Eng.*, 2015, **3**, 406–412.
- 179 J. M. R. Gallo, D. M. Alonso, M. A. Mellmer and J. A. Dumesic, *Green Chem.*, 2013, **15**, 85–90.
- 180 H. J. Ruijsenaars, Purac Biochem B.V (NL), *US Pat*, 2018/0030488A1, 2018.
- 181 S. M. Thomas, R. DiCosimo and V. Nagarajan, *Trends Biotechnol.*, 2002, **20**, 238–242.
- 182 M. Krystof, M. Pérez-Sánchez, P. Domínguez de María and P. D. De María, *ChemSusChem*, 2013, **6**, 826–830.
- 183 P. D. Hanke, *US Pat*, 2009/023174A2, 2009.
- 184 F. Koopman, N. Wierckx, J. H. de Winde and H. J. Ruijsenaars, *Bioresour. Technol.*, 2010, **101**, 6291–6296.
- 185 W. P. Dijkman, C. Bindu, M. W. Fraaije and A. Mattevi, *ACS Catal.*, 2015, **5**(3), 1833–1839.
- 186 C. F. Yang and C. R. Huang, *Bioresour. Technol.*, 2016, **214**, 311–318.
- 187 G. S. Hossain, H. Yuan, J. Li, H.-D. Shin, M. Wang, G. Du, J. Chen and L. Liu, *Appl. Environ. Microbiol.*, 2017, **83**, e2312–e2316.
- 188 H. Yuan, J. Li, H. Shin, G. Du, J. Chen, Z. Shi and L. Liu, *Bioresour. Technol.*, 2018, **247**, 1184–1188.
- 189 N. Wierckx, F. Koopman, H. J. Ruijsenaars and J. H. de Winde, *Appl. Microbiol. Biotechnol.*, 2011, **92**, 1095–1105.
- 190 C. Martin, A. Ovalle Maqueo, H. J. Wijma and M. W. Fraaije, *Biotechnol. Biofuels*, 2018, **11**, 56.
- 191 J. Carro, E. Fernández-Fueyo, C. Fernández-Alonso, J. Cañada, R. Ullrich, M. Hofrichter, M. Alcalde, P. Ferreira and A. T. Martínez, *Biotechnol. Biofuels*, 2018, **11**, 86.
- 192 Y. Wang, C. A. Brown and R. Chen, *AIMS Microbiol.*, 2018, **4**, 261–273.

- 193 H. G. Cha and K.-S. Choi, *Nat. Chem.*, 2015, **7**, 328–333.
- 194 R. Ciriminna, G. Palmisano and M. Pagliaro, *ChemCatChem*, 2015, **7**, 552–558.
- 195 W.-J. Liu, L. Dang, Z. Xu, H.-Q. Yu, S. Jin and G. W. Huber, *ACS Catal.*, 2018, **8**, 5533–5541.
- 196 N. Jiang, B. You, R. Boonstra, I. M. Terrero Rodriguez and Y. Sun, *ACS Energy Lett.*, 2016, **1**, 386–390.
- 197 K.-S. Choi and H. G. Cha, *US Pat*, 9598780B2, Wisconsin Alumni Research Foundation (US), 2017.
- 198 R. Latsuzbaia, R. Bisselink, A. Anastasopol, H. van der Meer, R. van Heck, M. S. Yagüe, M. Zijlstra, M. Roelandts, M. Crockatt, E. Goetheer and E. Giling, *J. Appl. Electrochem.*, 2018, **48**(6), 611–626.
- 199 S. Zhang and L. Zhang, *Pol. J. Chem. Technol.*, 2017, **19**, 15–20.
- 200 F. R. Duke and T. W. Haas, *J. Phys. Chem.*, 1961, **65**, 304–306.
- 201 L. Zhang, X. Luo and Y. Li, *J. Energy Chem.*, 2018, **27**, 243–249.
- 202 Avantium, YXY® technology, <https://www.avantium.com/yxy/yxy-technology/>.
- 203 B. Blank, A. Gordillo, M. A. Bohn, A. Kindler, S. A. Schunk, L. Zhang, C. Futter, R. Dehn, H. Werhan, J. H. Teles, M. Piepenbrink and R. Backes, Basf Se, *WO* 2015197699A1, 2015.
- 204 A. Gordillo, H. Werhan, R. Dehn, B. Blank, J. H. Teles, S. Schunk, M. Piepenbrink, R. Backes, L. Zhang and B. Se, *WO* 2017012842A1, 2017.
- 205 Mercurius Biorefining, <http://www.mercuriusbiofuels.com/index.html> (accessed 24 September 2018).
- 206 Bioplastics, <https://www.corbion.com/bioplastics/fdca> (accessed 24 September 2018).
- 207 Eastman Licenses 2,5-Furandicarboxylic Acid (“FDCA”) Technology to Origin Materials, [https://www.eastman.com/Company/News\\_Center/2017/Pages/Eastman-Licenses-2-5-Furandicarboxylic-Acid.aspx](https://www.eastman.com/Company/News_Center/2017/Pages/Eastman-Licenses-2-5-Furandicarboxylic-Acid.aspx) (accessed 20 September 2018).
- 208 M. Janka, D. Lange, M. Morrow, B. Bowers, K. Parker, A. Shaikh, L. Partin, J. Jenkins, P. Moody, T. Shanks and C. Sumner, *US Pat*, 20150011783A1, Eastman Chemical Company, Kingsport, TN (US), 2015.
- 209 Origin Materials, <https://www.bincanada.ca/single-post/2017/09/26/Origin-Materials-Announces-their-Oxidation-Pilot-Plant-will-be-located-at-The-Western-Sarnia-Lambton-Research-Park> (accessed 20 September 2018).
- 210 DuPont industrial biosciences, <http://biosciences.dupont.com/news/dupont-industrial-biosciences-and-adm-announce-breakthrough-platform-technology-for-long-sought-aftre/> (accessed 21 September 2018).
- 211 A. Sanborn, *US Pat*, 9562028 B2, Archer Daniels Midland Co. (US), 2017.
- 212 K. Stensrud and P. Venkitasubramanian, *WO* 2014099438A2, Archer Daniels Midland Co. (US), 2013.
- 213 T. Kläusli, *Green Process. Synth.*, 2014, **3**, 235.
- 214 AVA Technology, <http://www.ava-biochem.com/pages/en/technology.php> (accessed 22 September 2018).
- 215 Kläusli, Biobased news, <http://news.bio-based.eu/klaeusli-ava-biochem-the-bioeconomy-is-the-biggest-chance-we-have-to-decarbonise-our-world/>.
- 216 J. Van Haveren, S. Thiagarajan and A. T. Morita, *US Pat*, 20150119588A1, Braskem SA (NL), 2015.
- 217 Novamont, <https://www.novamont.com/eng/read-press-release/k-mater-bi-fifth-generation/> (accessed 22 September 2018).
- 218 G. Borsotti and F. Digioia, Novamont SPA, *US Pat*, 20130137882A1, 2013.
- 219 G. Borsotti and F. Digioia, Novamont SPA, *WO Pat*, 2012017052A1, 2012.
- 220 B. G. Siqueira, R. B. De Menezes, C. R. K. Rabello and M. Gomes Jr. Petróleo Brasileiro -Petrobras SA (BR), *US Pat*, 9199957B2, 2015.
- 221 B. G. Siqueira, R. B. De Menezes, C. R. K. Rabello and J. M. Gomes, Petróleo Brasileiro S.A. - Petrobras (BR), *WO* 2015054756A1, 2015.
- 222 Daniel Moran, <https://biorrefineria.blogspot.com/2017/10/vtt-releases-its-last-results-in-bioplastics-FDCA-Furandi-carboxylic-acidmuconic-acid.html> (accessed 24 September 2018).
- 223 VTT Green plastics, <https://makingoftomorrow.com/green-plastics-without-the-bio-premium/> (accessed 24 September 2018).
- 224 H. Boer, S. Hildich, P. Richard and M. Penttilä, Valtion Teknillinen Tutkimuskeskus (VTT), *WO* 2010072902A1, 2010.
- 225 D. Thomas, M. Asikainen and A. Harlin, Teknologian Tutkimuskeskus Vtt Oy, *WO* 2015/189481 A1, 2015.
- 226 WARF, <https://www.warf.org/technologies/clean-technology/solar-technologies/summary/solar-cells-turn-hmf-to-valuable-platform-molecules-p150132us01.cmsx> (accessed 24 September 2018).